STATUS OF THESIS

Application of SeaBed Logging (SBL) technology to Support 3D Seismic and AVO Analysis in Identification of Hydrocarbon

I, **WONG ENG YAO** hereby allow my thesis to be placed at the Information Resource Center (IRC) of Universiti Teknologi Petronas (UTP) with the following conditions:

1. The thesis becomes the property of UTP
2. The IRC of UTP may make copies of the thesis for academic purposes only
3. The thesis is classified as

☒ Confidential

☐ Non confidential

Endorsed by

Wong Eng Yao

Kamal Azlan Abdul Ghaffar

UNIVERSITI TEKNOLOGI PETRONAS

Approval by Supervisor

The undersigned certify that they have read, and recommend to The Postgraduate Studies Programme for acceptance, a thesis entitled "**Application of SeaBed Logging (SBL) technology to Support 3D Seismic and AVO Analysis in Identification of Hydrocarbon**" submitted by **Wong Eng Yao** for the fulfillment of the requirements for the degree of Master of Petroleum Geoscience.

Date 29.1.2008

Signature:

Main supervisor: Kamal Azlan Abdul Ghaffar

Date: 29.1.2008

UNIVERSITI TEKNOLOGI PETRONAS

Application of SeaBed Logging (SBL) technology to Support 3D Seismic and AVO Analysis in Identification of Hydrocarbon

By

WONG ENG YAO

A THESIS

SUBMITTED TO THE POSTGRADUATE STUDIES PROGRAMME

AS A REQUIREMENT FOR THE

DEGREE OF MASTER OF SCIENCE IN PETROLEUM GEOSCIENCE

BANDAR SERI ISKANDAR,

PERAK

JANUARY, 2008

DECLARATION

I hereby declare that the thesis is based on my original work except for quotations and citations which have been duly acknowledged. I also declare that it has not been previously or concurrently submitted for any other degree at UTP or other institutions.

Signature : 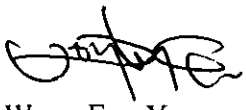

Name : Wong Eng Yao

Date : 29.1.2008

ABSTRACT

SeaBed Logging (SBL) method came into oil and gas exploration industry and provides geoscientists another tool to explore a prospect by looking at another physical property, i.e. resistivity, besides acoustic impedance that can be obtained from seismic and AVO analysis. SBL technology is no doubt a tool to complement seismic interpretation and AVO analysis by offering an independent data set to exploration works. However, as the technology is purely based on resistivity contrast down-earth, there're still rooms for discussion to validate whether or not the technology is capable enough to help in delineating the true geology of an area.

This study presents the result of a 2D SBL survey over 2 deep water prospects, Prospect A and Prospect B, in Block 2F, Rajang Delta, offshore Sarawak. These 2 prospects represent 2 cases that show different seismic interpretation in terms of amplitude anomalies and different AVO analysis responses. The 3D seismic and AVO analysis of Prospect A do not show any amplitude anomaly at the crest of the structure but at the flank of the structure. Meanwhile for Prospect B, 3D seismic shows a high amplitude anomaly at both crest and flank sides of the structure; and a Class III AVO response showed in the AVO analysis over the crest of Prospect B.

The result of SBL survey over both Prospect A and Prospect B are then collaborated to the seismic interpretation and AVO analysis. It is clearly showed that the SBL responses matches well with the high amplitude features seen in seismic and AVO analysis of Prospect B; and SBL only shows weak response in the case where both seismic and AVO analysis hardly show anything like in Prospect A.

TABLE OF CONTENTS

LIST OF FIGURES

1. CHAPTER 1: GEOLOGICAL INTRODUCTION

Rajang Delta is located in the province of West Luconia, Sarawak Basin, Malaysia. Figure 1.1 illustrates the location of Rajang Delta in Sarawak Basin and the outline of Block 2F inside. The Sarawak Basin is a foreland basin that formed after the collision of the Luconia Block with the West Borneo Basement, and the closing of the Rajang Sea during the Late Eocene (Mazlan Hj. Madon, 2007).

Block 2F is situated in a toe-thrusting realm of Rajang Fold-Thrust Belt that formed after two phases of tectonic deformation occurred during Oligocene-Early Miocene and Middle Miocene-present day, which are known as foreland basin phase and passive margin phase respectively. Foreland basin phase featured a rapid subsidence of Sarawak margin and northwestward thrusting of the Rajang Group accretionary prism. The passive margin phase of tectonic deformation featured a gradual subsidence of the Sarawak margin, accompanied by extensional, wrench faulting, and toe-thrusting in different parts of the margin (Mazlan Hj. Madon, 2007; Theresia Heru Kuswardhany *et al.* 2006).

The reservoirs of Block 2F were mainly deposited during the age of late Miocene to early Pliocene, which is during the passive margin phase of continental margin evolution. The targeted 5.5sb and 8.2sb depositions are recognized as Basin Floor Fan (BFF) of middle Miocene age which is believed to be deposited before the local toe-thrusting event in Block 2F. Meanwhile, the horizons of 3.0sb and 3.8sb of late Miocene are deposited during the toe-thrusting event, hence it features ponded turbidites that thickened at the epicenter of trough and pinched out towards the flanks of the trough. The locations of case studies prospects are showed in Figure 1.2.

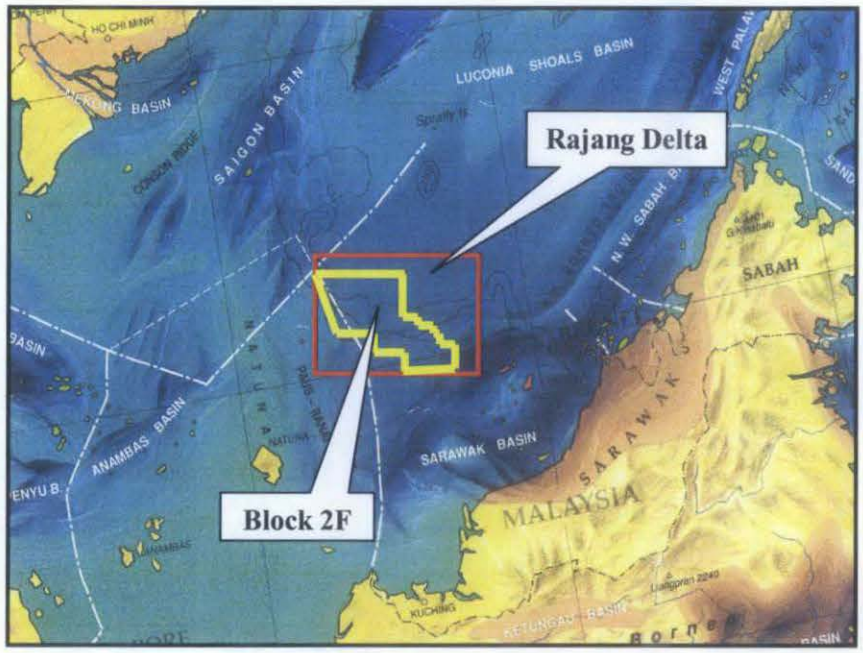

Figure 1.1: The location of Rajang Delta in Sarawak Basin and the outline of Block 2F (yellow outline).

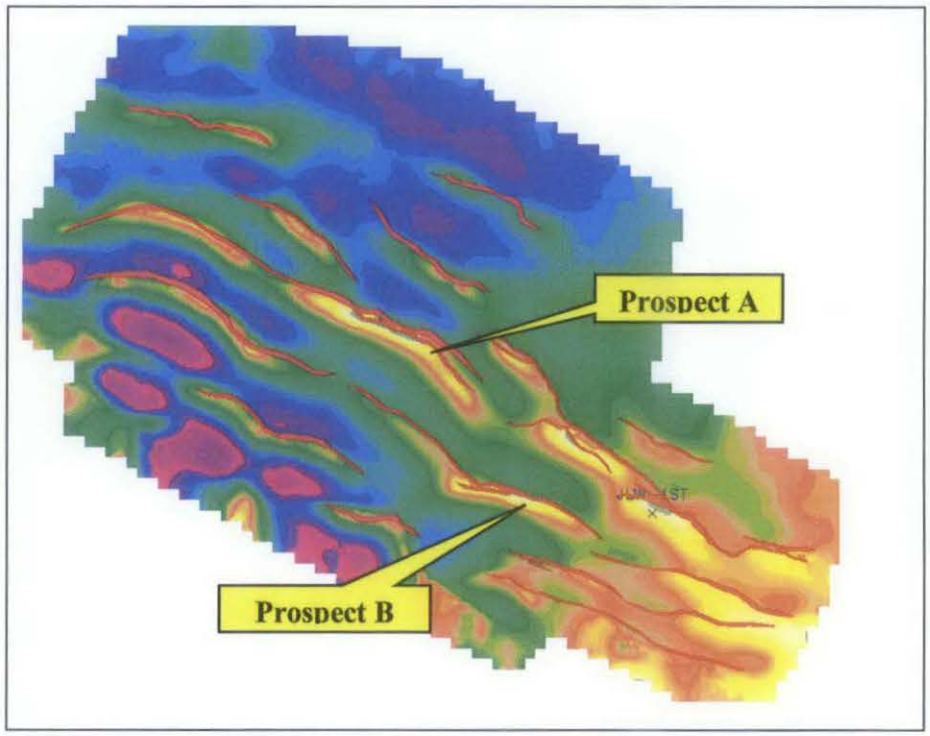

Figure 1.2: The location of Prospect A and Prospect B in Block 2F (adapted from Theresia Heru Kuswardhany *et al*. 2006).

2. CHAPTER 2: SEABED LOGGING (SBL): INTRODUCTION AND THE THEORY BEHIND

SeaBed Logging (SBL) is an application of controlled-source electromagnetic (CSEM) sounding which has been introduced in the 1980s. After 20 years of development and evolution, SBL is now a proven technology method for remote and direct identification of hydrocarbon-charged reservoirs in water depths ranging from 250 – 3000 m.

As the nature of SBL technique is the detection of resistivity contrast, the technology is not only limited to identify HC bearing layer but it also helps to map the resistive bodies lain beneath earth surface, such as basalt sills, carbonate structures, tight formation, and shallow gas. It aids tremendously in imaging of sub-basalt and sub-salt geology (Chopra *et* al. 2007; MacGregor, 2007).

In exploration point of view, with the integration of the other survey method such as seismic, SBL technology is used to substantially reduce drilling risk and in addition can resolve challenges related to the following:

a) Direct Identification of a Potential Hydrocarbon Reservoir
b) Prospect Ranking
c) Adjacent Prospect Evaluation
d) Reservoir Delineation
e) Farm-In/ Farm-Out Decision Tool

.

(EMGS, 2005)

2.1 Introduction

The basic idea behind SBL is to detect the resistivity contrast between water-bearing formations and hydrocarbon-bearing formations. The resistivity difference between water-saturated shale and sandstone is usually small (1-2 Ωm), but resistivity of a reservoir increases to 10 to 500 Ωm if it is saturated with oil or gas (Chopra *et al.* 2007). Identification of hydrocarbon by SBL technique hence is done based upon the high resistivity contrast.

While traditional exploration methods use acoustic waves to obtain information about subsurface lithology, SBL method uses electromagnetic (EM) energy. The source of electromagnetic energy used in SBL survey is called Horizontal Electric Dipole (HED) source. HED transmits ultra low frequency (a few tenths to a few tens of Hz) EM signal that diffuses outwards into the overlying water column and downwards into the seabed (Eidesmo *et al.* 2002).

The mathematical theory behind this technology is based on Maxwell's equations. Maxwell's equations comprise of 4 equations that define the relationship among electric field ($\vec{E}$), magnetic field ($\vec{B}$), magnetic field strength ($\vec{H}$) and electric displacement field ($\vec{D}$).

Ampere's Law: $$\nabla \times \vec{E} + \frac{\partial \vec{B}}{\partial t} = 0$$

Faraday's Law: $$\nabla \times \vec{H} - \frac{\partial \vec{D}}{\partial t} = \vec{J}(\vec{r})$$

Gauss' Laws: $$\nabla \bullet \vec{D} = \rho(\vec{r})$$

$$\nabla \bullet \vec{B} = 0$$

Where $\vec{E}$ = electric field;

$\vec{B}$ = magnetic field;

$\vec{H}$ = magnetic field strength;

$\vec{D}$ = electric displacement field;

$\vec{J}$ = current density; and

ρ = resistivity

In brief, Ampere's Law expresses how electric currents and changing electric fields produce magnetic fields and Faraday's Law explains how changing magnetic fields produce electric fields while Gauss' Laws explain how electric charges produce electric fields.

The decay rate of EM is mathematically termed as

$$e^{(-z/\delta)}$$

where z is distance (m);

$$\delta = \left[\frac{2\rho}{(8\times10^{-7})\pi^2 f}\right]^{\frac{1}{2}}, \quad \rho \text{ is resistivity } (\Omega\,\text{m}); f \text{ is frequency (Hz)}$$

The mathematic equation explains that the EM energy attenuates exponentially in a conductive medium (of low ρ) and attenuates exponentially with distance, z.

Distance z is a parameter of skin depth. Skin depth is a distance required to attenuate an EM signal by the factor of e^{-1} which equals to 0.37. For instance, by using an acquisition frequency of 0.25 Hz, the skin depth is about 551 m in seawater (0.3 Ω m), 1424 m in a 2-Ω m sediment, 10^4 m in HC bearing sediment (100 Ω m) and 10^8 m in air (10^{10} Ω m). (Johansen *et al.* 2005).

The application of EM signal's decay rate and calculation of skin depth shown above simply indicates that in a relatively thin (20-200 m) and resistant layer, i.e. HC bearing layer, EM energy will be attenuated less and be guided along the high resistivity layer under a critical angle. The guided energy will constantly be reflected back to the EM receivers laid on sea bed and recorded as an altered pattern of current flow in overburden layers. (Eidesmo *et al.* 2002; Johansen *et al.* 2005). Figure 2.1 illustrates the components of EM signal and their respective ray paths from HED source to EM receivers. Guided energy is also known as guided wave. Total reflection happens if the transmitted energy enters the high resistivity interface with incidence angle greater than critical angle. In this case, direct reflected energy from the HC bearing reservoir will be recorded.

Besides guided wave which is refracted and guided along subsurface high resistivity layer, there's energy that is reflected and refracted via the air-water interface which we call airwave. Airwave is a signal component that traverses upward from the HED source to sea surface, traverses horizontally along sea surface without attenuation, and then traverses back downward through water column to receiver.

Air wave is a common masking problem in shallow water and at long source-receiver offset. It happened due to the extreme velocity contrast at water-air interface. The critical angle at the interface is almost 90^{o} and transmitted energy with normal incidence will traverse along the interface, while for transmitted energy that enters the interface with incidence angle greater than 90^{o} will tend to be totally reflected which we call surface reflection energy (Amundsen *et* al. 2006). Lower acquisition frequency and higher water depth will give less masking problem of air wave (Eidesmo *et al.* 2002). However, a few processing algorithms have been developed to handle the air wave masking problem, this includes Up-down Separation, and Surface Related Multiple Elimination (SRME) technique.

Another component of EM signal is direct field which is transmitted directly from HED source to EM receiver. The direct field dominates in amplitude strength at short source-receiver offset but not at long source-receiver offset (Amundsen *et* al. 2006).

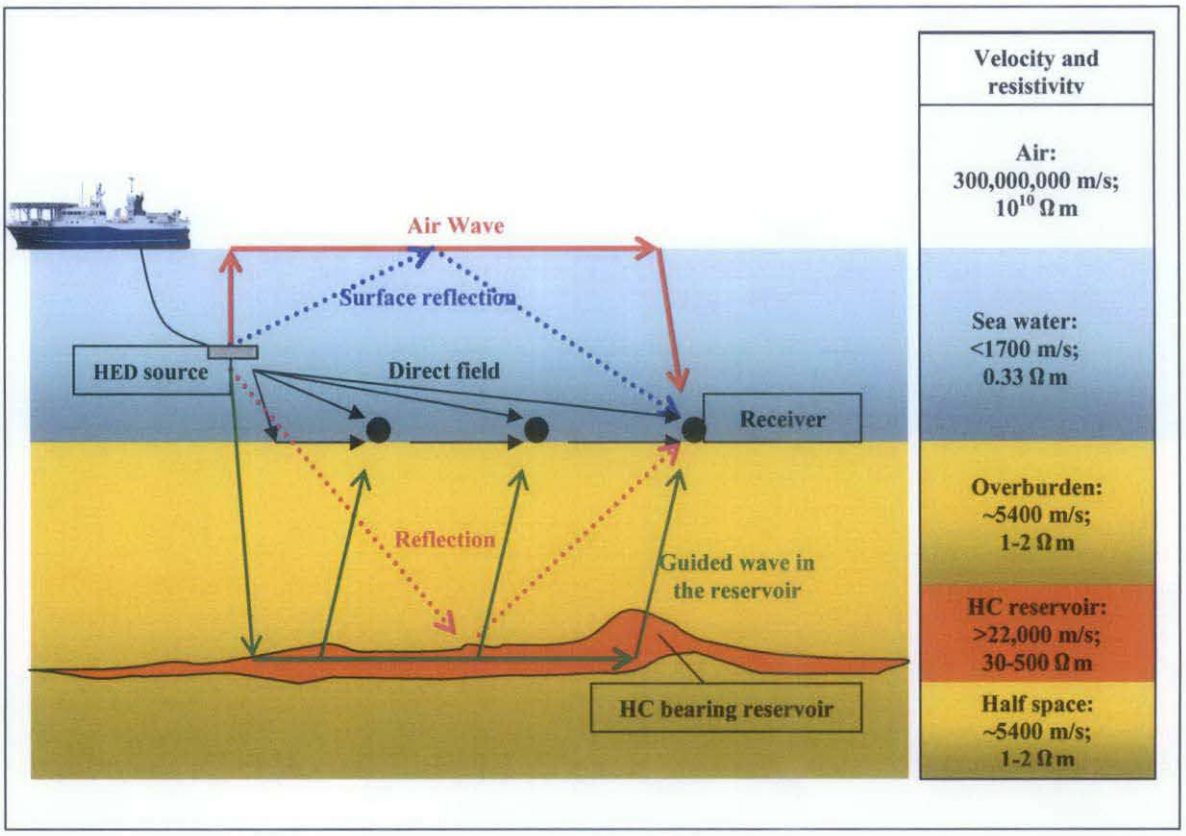

Fig 2.1: Various EM signal's components and their respective ray paths. Right panel of the figure shows the velocity and resistivity of each layer of transmitting medium.

2.2 SBL Responses

It is crucial to understand the SBL responses from the components of EM signal. There are two types of plot that is fundamental for SBL data interpretation: magnitude and phase.

2.2.1 Magnitude versus Offset and Normalized Magnitude versus Offset

A plot of electric magnitude ($VA^{-1}m^{-2}$) versus source-receiver offset (m), also known as Magnitude versus Offset (MvO) plot is used to visualize the attenuation of the responding electromagnetic wave from the resistive body underneath. As mention above, high resistivity layer will tend to attenuate less compare to low resistivity layer; hence, an MvO plot is always plotted in relative to the response from background resistivity in order to display the contrast. Normalize Magnitude versus Offset (NMvO) is a straightforward way to visualize the contrast

between background resistivity response and anomaly response. Figure 2.2 and Figure 2.3 show examples of MvO and NMvO. The plotting of MvO and NMvO will be discussed later.

In an NMvO plot, a resistivity anomaly will show a build-up with normalized magnitude more than 1. For the response with normalized magnitude equals to 1, it refers to the background resistivity or reference resistivity as seen in Figure 2.3.

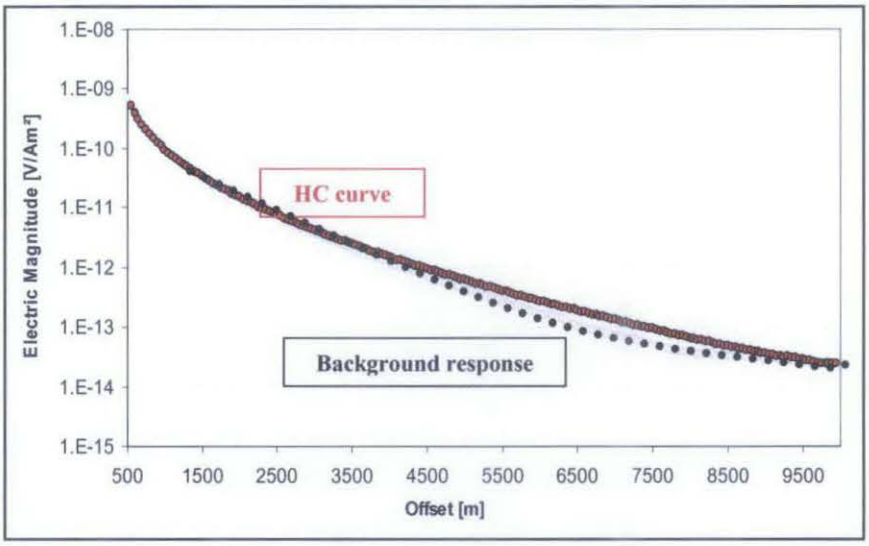

Figure 2.2: Electric magnitude versus Offset (MVO) profile from a typical SBL survey. The red curve shows the response from subsurface resistor and the white curve shows the response from background or reference resistivity.

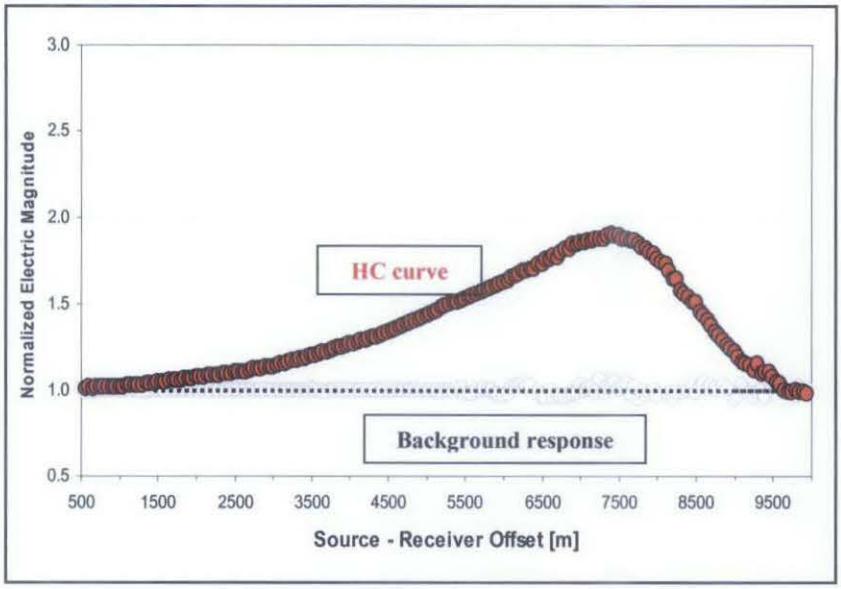

Figure 2.3: Normalized Electric magnitude versus Offset (MVO) profile from a typical SBL survey. The red curve shows the response from subsurface resistor and the white curve shows the response from half space. The background response has been used as a reference model for normalization.

2.2.2 Phase versus Offset and Phase Difference versus Offset

Another plot for SBL study is the phase plot. Gradient of a phase plot indicates the phase velocity of propagating EM field. Different components of wave have different phase velocities. Basically, an EM wave that has been guided along a resistive body will have lower phase velocity due to the increment of propagating velocity; while air wave, on the other hand, has a relatively higher phase velocity. The function of the parameter is presented as gradient in a plot known as Phase (degree) versus Offset (m), PvO in short, and it's showed in Figure 2.4 below.

In PvO, a curve that is less steep (smaller gradient) than reference curve is considered as a response curve that derived from resistive body. The trend of a phase plot shows the airwave condition of the survey. A 'roll-over' trend seen in Figure 2.4 indicates that air-wave effect starts to dominate the EM response. A normalized PvO plot is called Phase Difference versus Offset (PDvO), showed in Figure 2.5.

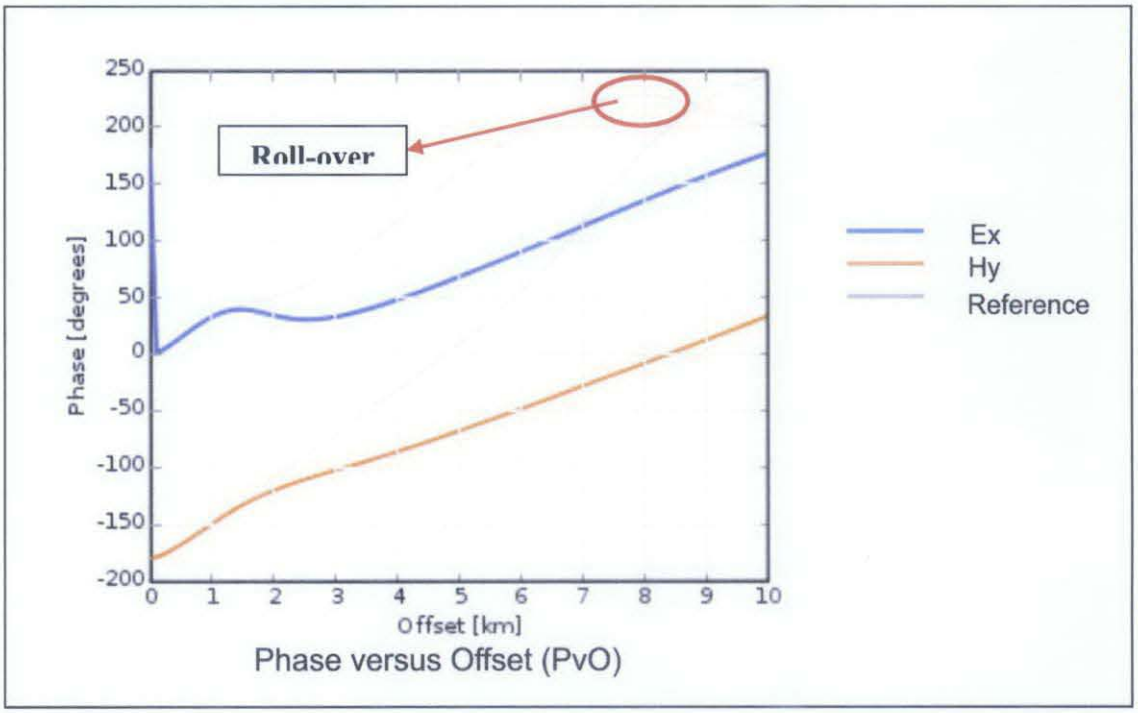

Figure 2.4: Phase versus Offset (PvO) plot from a typical SBL survey. The red and blue curves are the responses from subsurface resistor, for the electric and magnetic field, respectively, and the white curve shows the response from background or reference resistivity. A roll-over feature indicates that air-wave starts to dominate the survey.

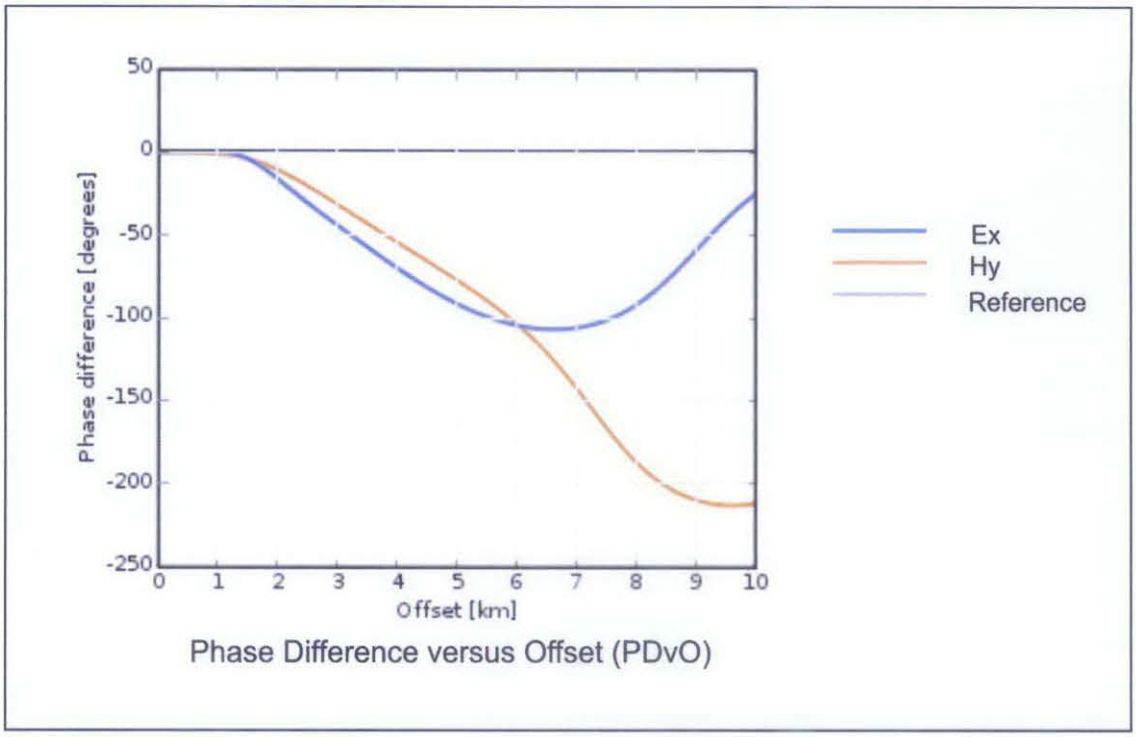

Figure 2.5: Phase Difference versus Offset (PDvO) plot from a typical SBL survey. The red and blue curves are the responses from subsurface resistor, for the electric and magnetic field respectively, and the white curve shows the response from background or reference resistivity.

3. CHAPTER 3: FROM RAW DATA TO SUMMARY PLOT: PROCESSING OF SBL DATA

The electrical field (E) will be recorded by 4 channels (Ex1, Ex2, Ey1 and Ey2) while the magnetic (H) field will be recorded by magnetic coils (Hx1 and Hy1) for each SBL receiver in data acquisition phase. The processing of the data, on the other hand, is aimed at reviewing the quality of the data from each channel, and summing or filtering the data of same field and same direction in order to eliminate the noise of the data.

The processing workflow is rather straightforward. Flowchart shown in Figure 3.1 indicates the basic workflow of SBL data processing.

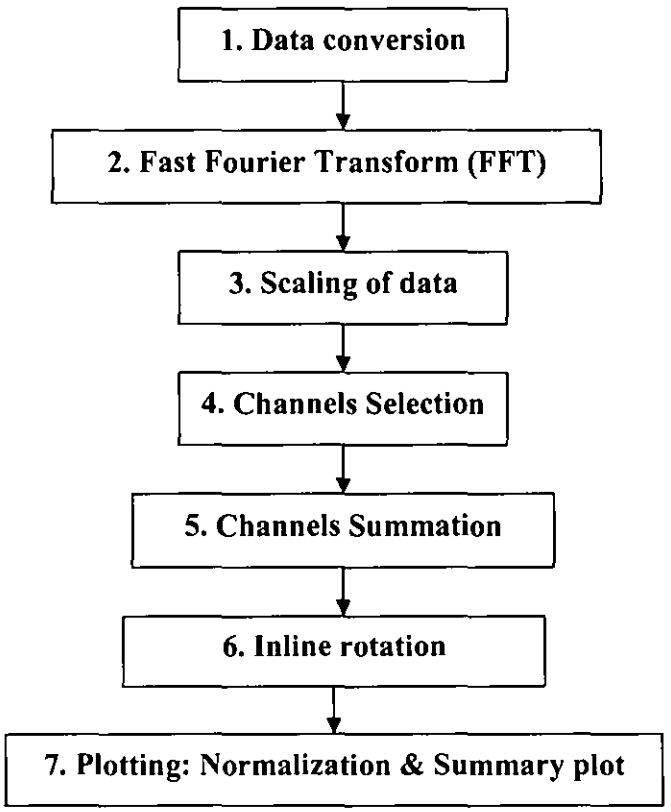

Figure 3.1: SBL data processing workflow.

3.1 Data Conversion, Fast Fourier Transform (FFT), and Scaling of Data

As the data processing is done in frequency domain while the data is acquired and stored as time series, data conversion and Fast Fourier Transform are performed to convert into the right format for data processing. These two steps of data processing are normally done on acquisition vessel; right after the data is acquired from the field.

The data is then scaled to phase or amplitude data depending on the processing algorithm needed. Scaling to phase data is to subtract the phase data of source in order to honor fully phase data of responding EM field. On the other hand, scaling to amplitude data is aimed to compensate the variation of source current amplitude and to simplify the amplitude data according to modeled source data (pers comm.: Tor Atle Wicklund).

3.2 Channels Selection and Channels Summation

As mentioned, there are 6 channels that record E-field and H-field in both X and Y directions, respectively, and two sets of Ex and Ey channels are used, i.e. Ex1, Ey1, and Ex2, Ey2, which provide us redundant measurements for the electric field.

The excess of E-channels in each receiver allows channels that record better data are taken into consideration for processing and modeling purposes. However, channels summation method allows both channels that record equivalent good electric data from the same direction, i.e. both Ex1 and Ex2 or Ey1 and Ey2, to be taken into account.

Figure 3.2 and Figure 3.3 below show 2 plots of data recorded by a receiver. Figure 3.2 illustrates a plot which the receiver's channels have not yet been summed up and Figure 3.3 shows the plot after channel summation. Note that the quantity of the E-channels' plots have been reduced after channel summation.

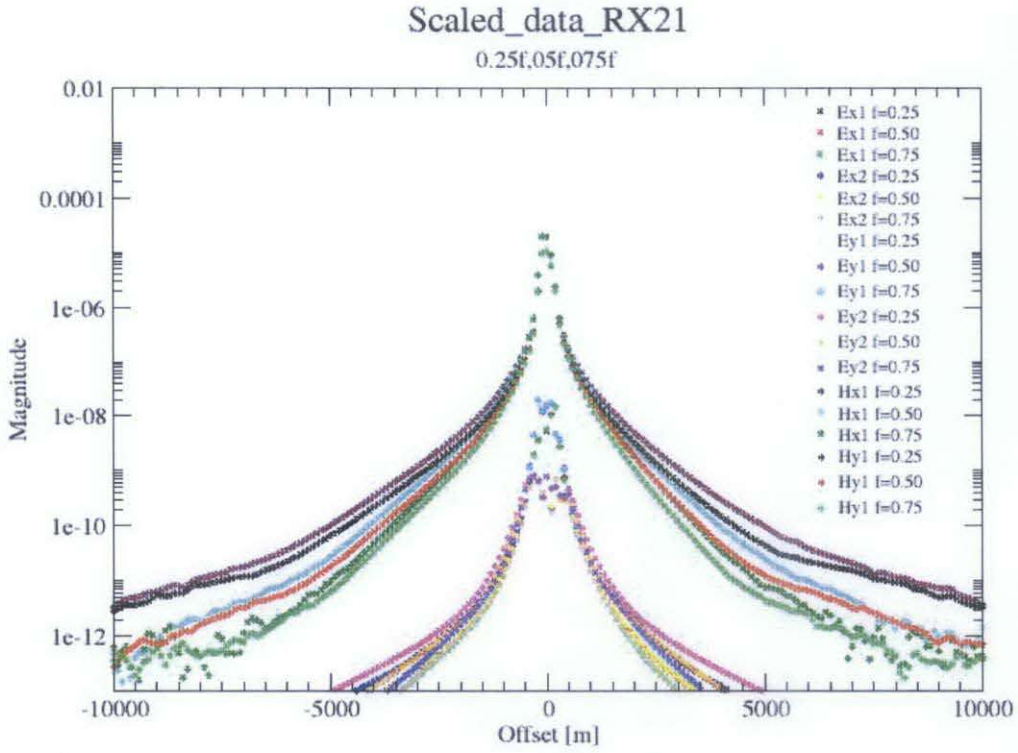

Figure 3.2: Plots of data before channel summation, recorded by Receiver 21 at frequency of 0.25Hx, 0.5Hz and 0.75Hz.

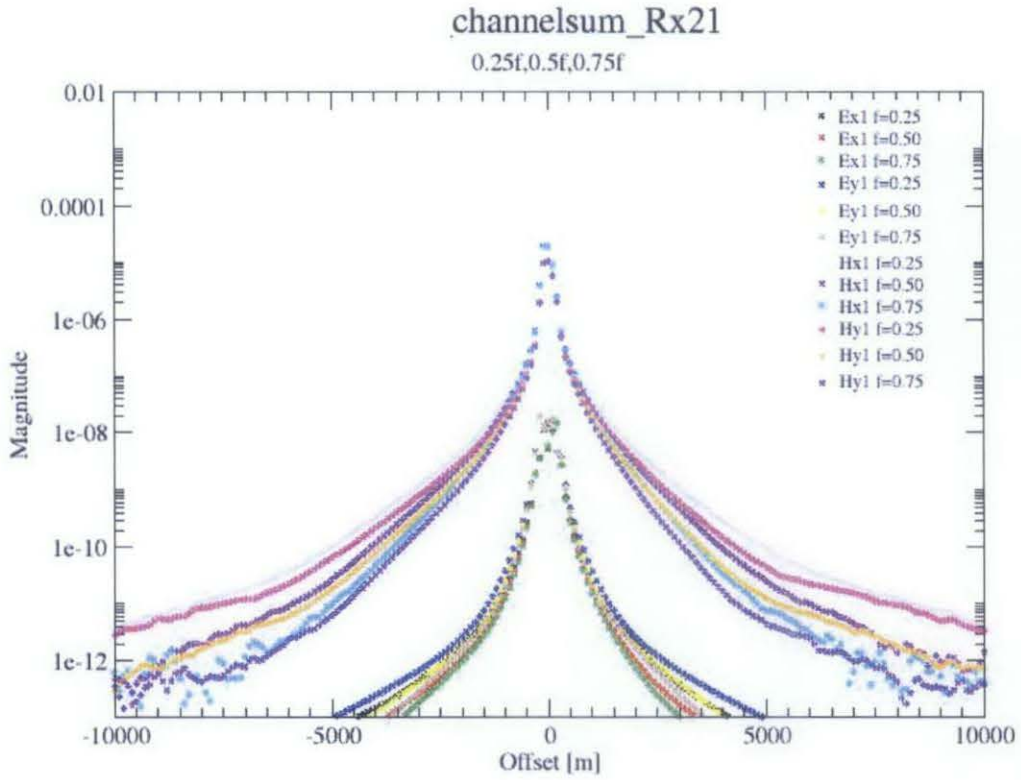

Figure 3.3: Plots of data after channel summation, recorded by Receiver 21 at frequency of 0.25Hx, 0.5Hz and 0.75Hz.

3.3 Inline Rotation

Inline is a source-receiver configuration where the fields are radial (parallel) to the line joining the source and the receivers. As EM field is a vector field and the receivers have arbitrary orientation on the seafloor, the data collected by all receivers need to be rotated into inline position in order to obtain the strongest measurement, which has better quality and defines the anomaly better. The angle of deviation of Ex channel from the inline direction will be calculated in order to perform inline rotation. The rotated data is the end product of data processing and it will be used in modeling and advanced imaging phase.

Figure 3.4 shows the plot of rotated data from the same receiver of Figure 3.2 and Figure 3.3. Apparent improvement of data quality on Ex and Hy channel is observed in the rotated plot.

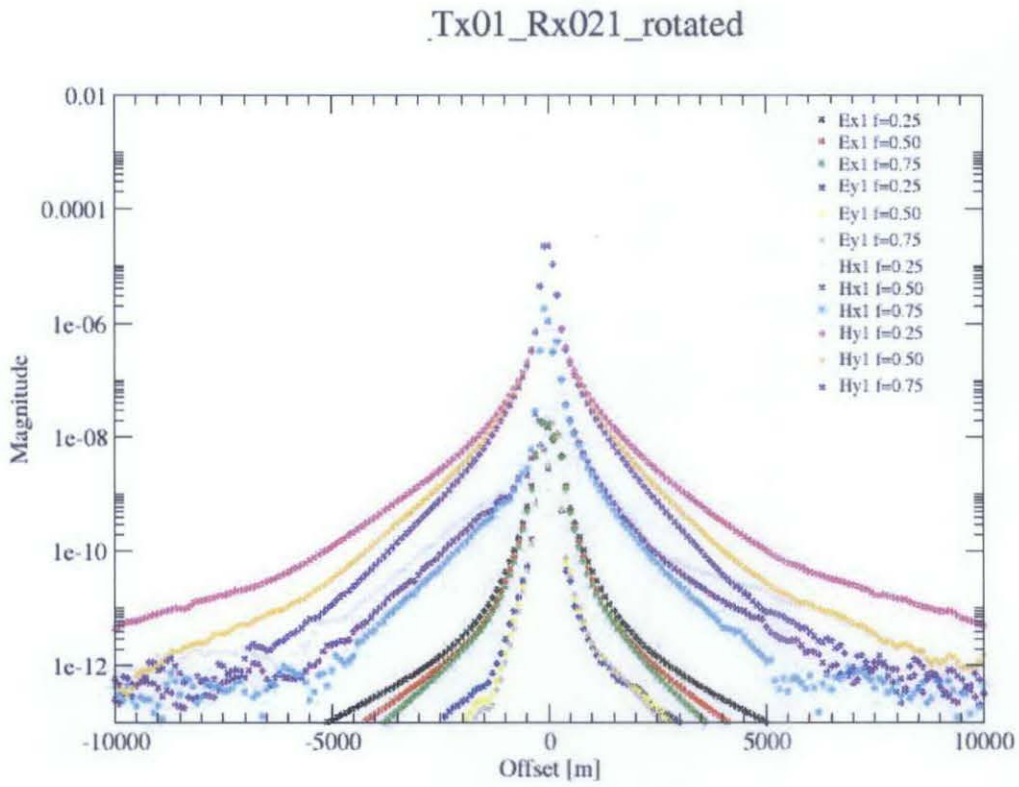

Figure 3.4: Plots of data after inline rotation, recorded by Receiver 21 at frequency of 0.25Hx, 0.5Hz and 0.75Hz.

3.4 Plotting

Plotting of SBL data is a presentation of the processed data in a meaningful way, in order to make interpretation possible. The plots, Magnitude versus Offset (MvO) plot and Phase versus Offset (PvO), are normally compared to a background model where no resistivity anomaly is expected. By having this comparison, the deviation in magnitude and phase of the data compared to of background model will be considered as responses due to resistivity anomaly or air-wave effect.

3.4.1 Normalization

In order to have a straightforward visual interpretation on the deviation, MvO and PvO will be normalized against the reference model or background model. A normalized plot of one receiver is a plot of its data against the data from the reference receiver which only measure background resistivity.

Normalized Magnitude versus Offset (NMVO) is plotted by dividing the magnitude of the collected data over the magnitude of the reference data. A normalized version of Phase versus Offset plot is better known as Phase Difference versus Offset (PDvO). As the name indicated, a PDvO is a plot showing the difference of phase data between a receiver and a reference receiver. Figure 3.5 shows simplified MvO and NMvO that are plotted according to a resistivity model at the left meanwhile Figure 3.6 illustrates a plot of PvO and its corresponding PDvO of the same resistivity model.

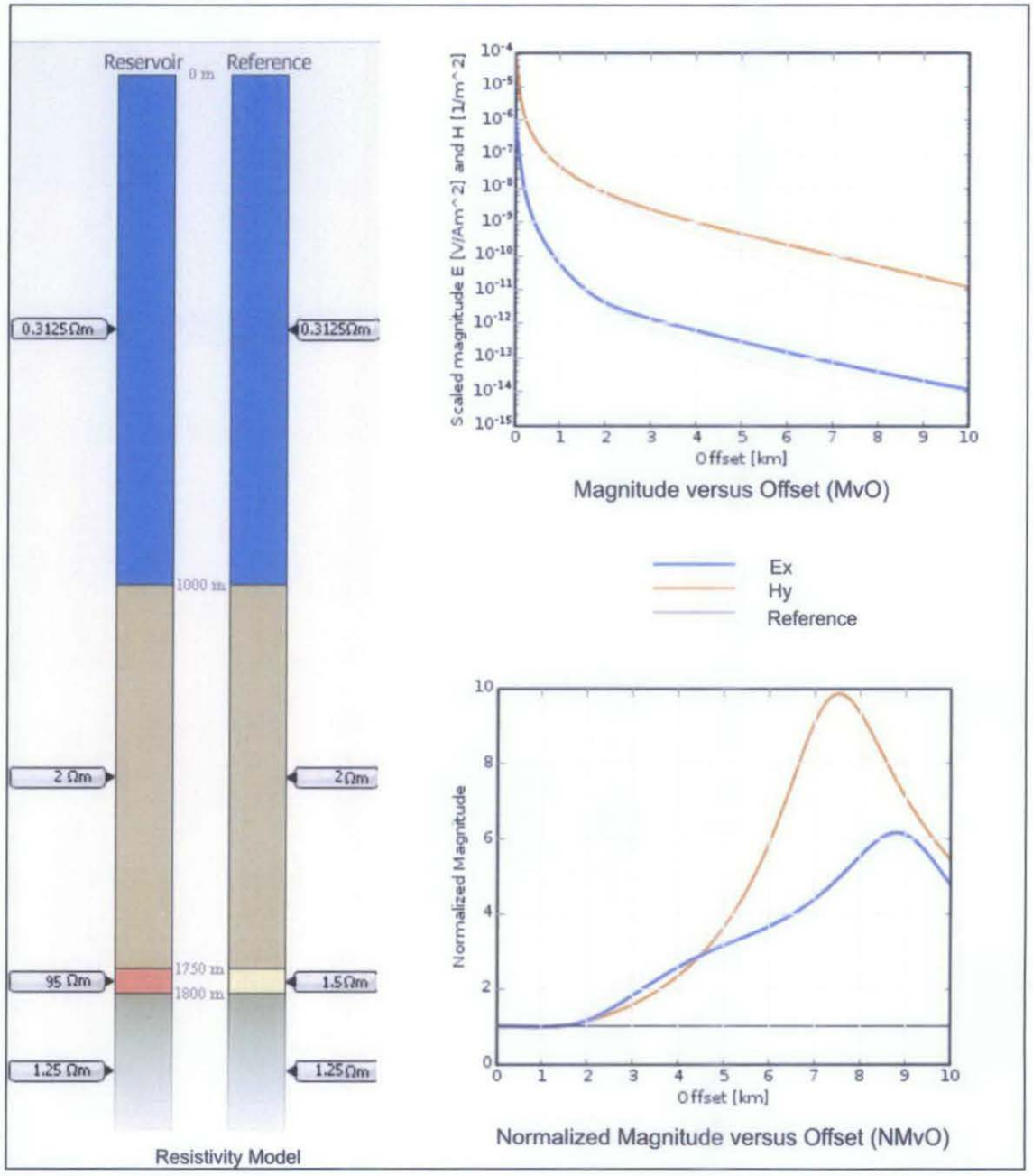

Figure 3.5: An MvO (right, above) and its corresponding NMvO (right, below) responding to a synthetic resistivity model at the left panel. The blue curve in the plots is electric response; the orange curve refers to magnetic response while the grey curve is the response of a background model (non-HC case).

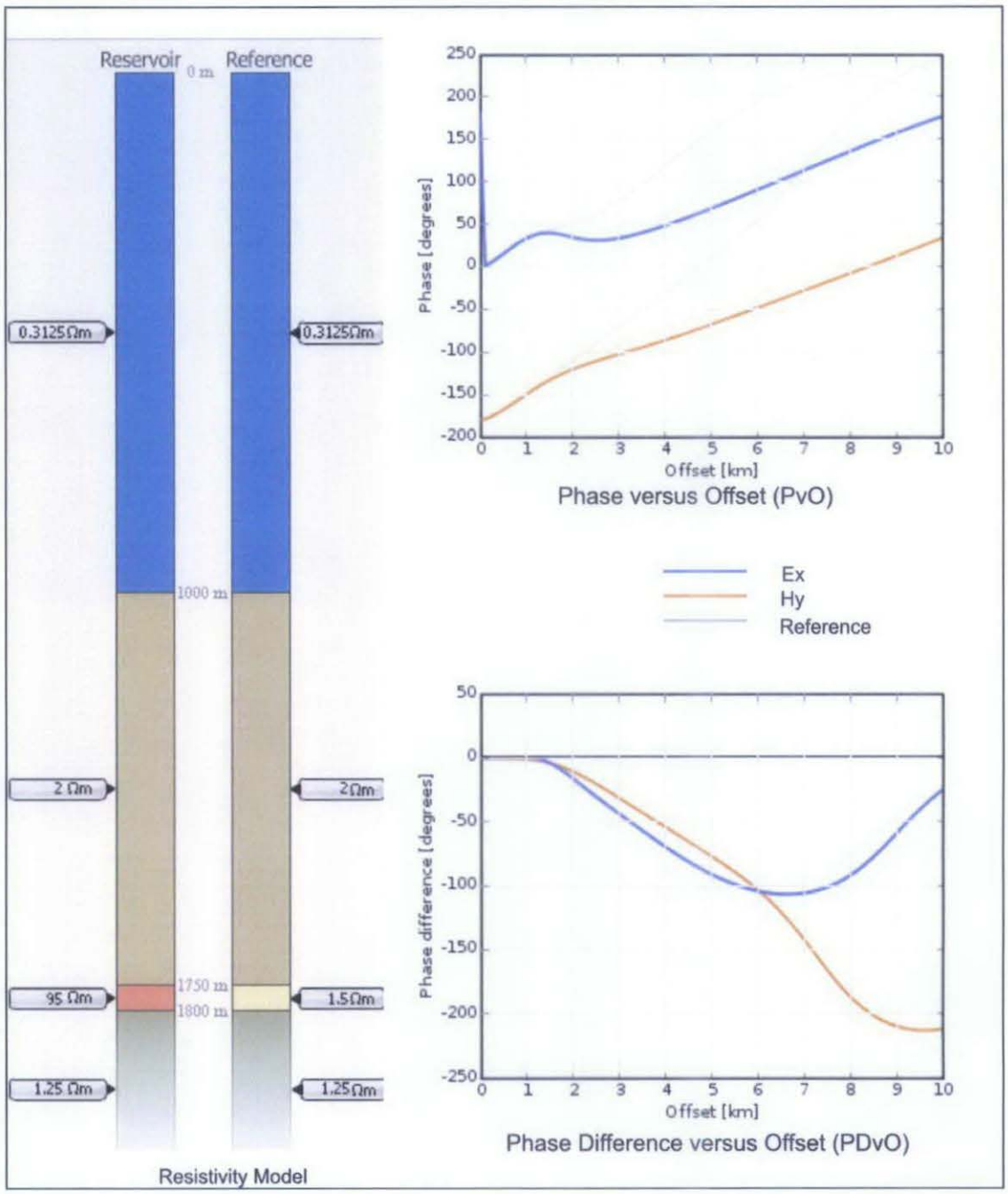

Figure 3.6: A PvO (right, above) and its corresponding PDvO (right, below) responding to a synthetic resistivity model at the left panel. The blue curve in the plots is electric response; the orange curve refers to magnetic response while the grey curve is the response of a background model (non-HC case).

3.4.2 Summary plot

Summary plot is a plotting approach that shows the response of every receiver along the survey line at one particular offset and frequency. It's rather convenient to visualize the anomaly response from the whole survey line. Moreover, as penetration depth is directly related to the offset between receiver and source, the depth of anomaly can be estimated by considering the offset of the plot, i.e. near offset refers to shallow depth; intermediate offset shows anomaly from intermediate depth, and so on. Nevertheless, the estimation of detection depth is still depending on the geology of the survey area.

Figure 3.7 shows a summary plot at intermediate offset. The plot shows both normalized magnitude and phase difference of every receiver along the survey line.

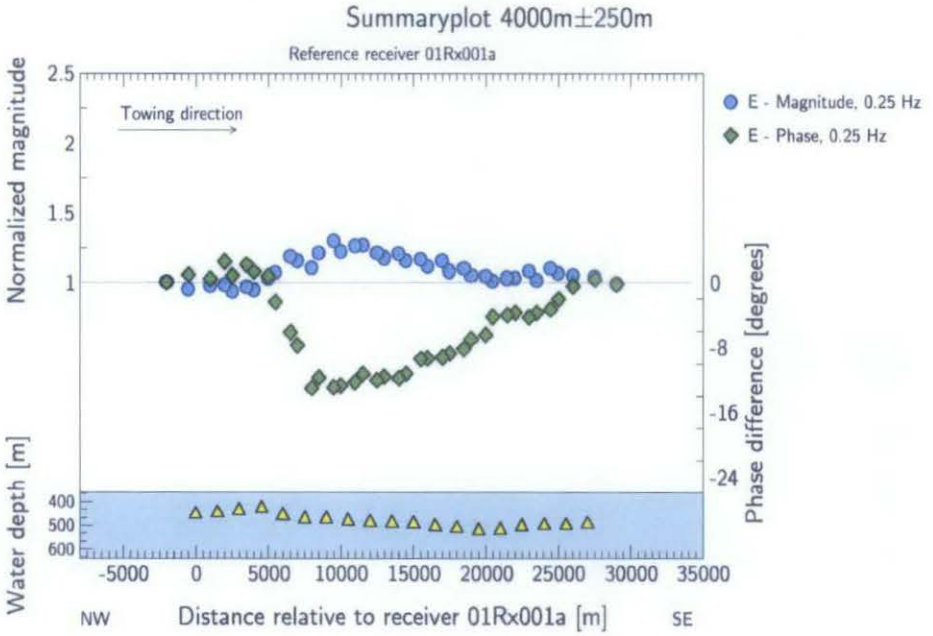

Figure 3.7: A summary plot at 4000m offset. Note that the magnitude and phase anomaly are detected from the 4th receiver to 17th receiver of the survey. The anomaly is detected at intermediate depth as indicated by the source-receiver offset of the plot.

4. CHAPTER 4: UP-DOWN SEPARATION

In most shallow water SBL surveys, receivers that lay on sea bed are not only detecting leakage of guided wave from resistive body beneath sea bed, strong refraction and reflection from sea surface will also go directly to the receivers and be recorded. This direct downward traveling wave from sea surface, categorized as down-going wave, may mask the responses from resistive body beneath sea bed and cause weak anomalies to observe.

Figure 4.1 shows the constituents of EM wave that will be received and recorded by SBL receivers. Air wave, surface reflection and direct field wave are down-going wave that will mask the response from up-coming wave from the resistive body beneath.

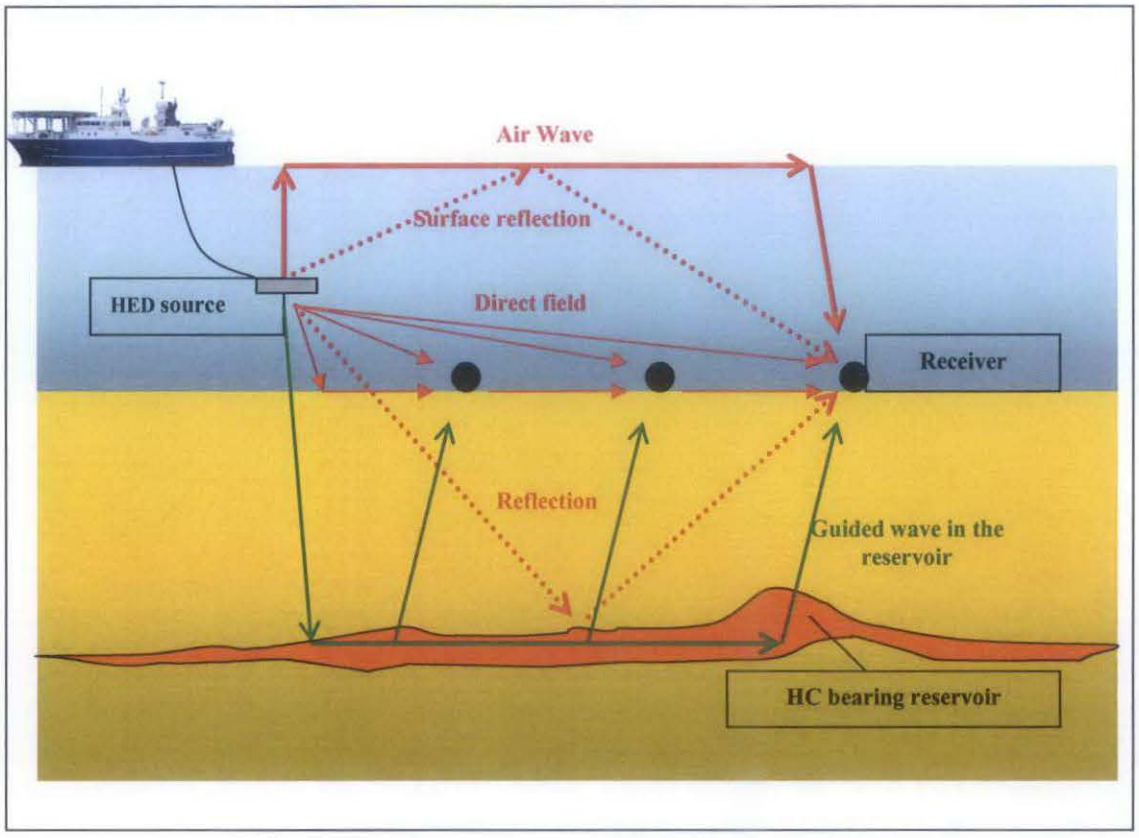

Figure 4.1: Up-going and down-going constituents of EM wave that will be detected and recorded by SBL receivers. The down-going wave (red path) will mask the up-going wave (green path) and cause weak anomalies to observe.

Up-down separation is an approach to remove the down-going wave from the data. To do that, electric and magnetic field is decomposed into up-going and down-going constituents. A general equation of decomposition of electric wave in X direction of each receiver is used here to explain the matter (Roth, F., 2007):

$$E_x^{(U)} = 0.5\left[E_x - (\sqrt{i\omega\mu_o\rho_{SF}})H_y\right]$$

Where E_x = Electric field in X-direction;

('U' in the superscript denotes '*Upgoing field)*';

H_y = Magnetic field in Y-direction;

$i = \sqrt{-1}$;

ω = Angular frequency;

μ_0 = Free space magnetic permeability;

ρ_{SF} = Sea floor resistivity, or top layer resistivity.

The same expression goes to the case of electric field in Y-direction. Note that the equation is simplified to 1D case where vertical traveling path of up- and down-going wave is taken into account (Amundsen, L., 2006).

As per described in the equation above, the resistivity of top formation or sea floor resistivity, ρ_{SF}, is particularly crucial in terms of estimating the true up-going component from electric field. The best-guessed ρ_{SF} is always needed to run up-down separation in order to enhance response of resistivity anomaly by up-going wave. Figure 4.2 shows a set of NMvO that have been up-down separated using various ρ_{SF}. Figure 4.2(a) is the plot of NMvO without performing up-down separation, while Figure 4.2(b) is the NMvO plot with the true ρ_{SF} for up-down separation.

Comparison can be made by observing the behavior of each plot using different sea floor resistivity to perform up-down separation. Normalized magnitude that is less that 1 indicates

air-wave effect and it's easily observed in Figure 4.2(a); and apparently after up-down separation, the airwave effect has been eliminated.

Wrong sea floor resistivity after up-down separation will show spiky anomalies as seen in Figure 4.2(c) and Figure 4.2(f). Spiky anomalies happen when only anomaly at certain source-receiver offset is enlarged but not for the rest of the offset distance. The valid up-down separation will give smooth and wide magnitude anomalies as seen in Figure 4.2(b), at all source frequency (Roth, F., 2007). This is important as for some up-down separation plots with a value of ρ_{SF}, the 'smooth and wide' anomaly profile happens only at a low source frequency but not for the higher ones. The inconsistency demotes the validity of the sea floor resistivity to be chosen for up-down separation. This can be observed in Figure 4.2(d) and Figure 4.2(f) in which both use the same sea floor resistivity but show different anomaly profile due to different source frequency.

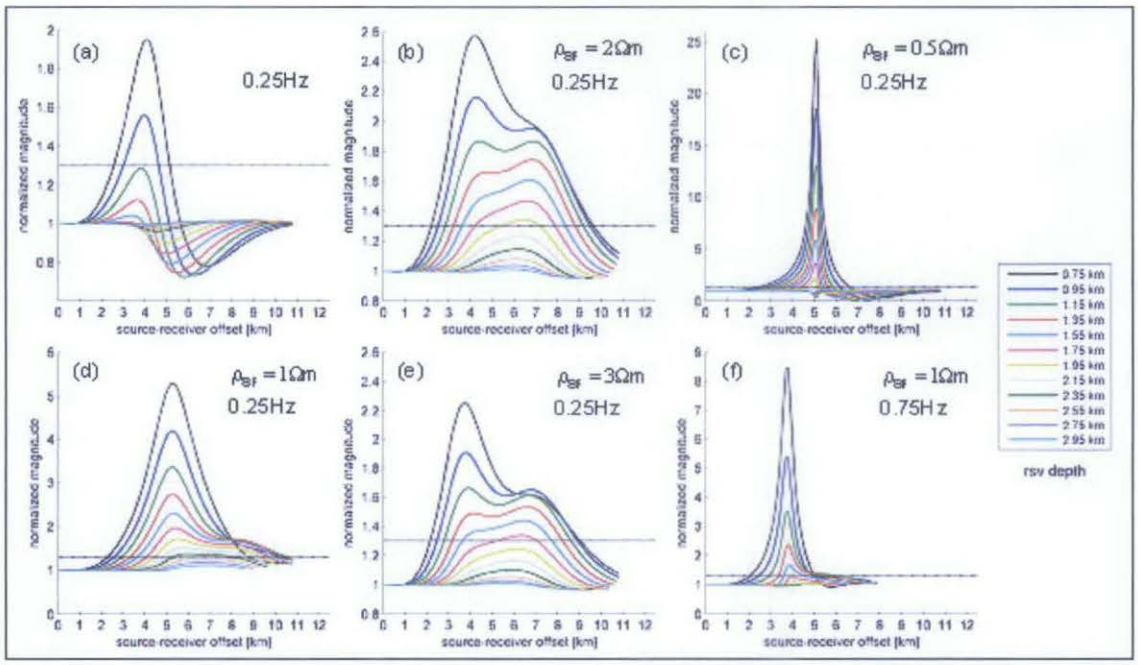

Figure 4.2: Set of NMvO plots. (a) NMvO without up-down separation; (b) NMvO with true sea floor resistivity for up-down separation; (c)-(f) NMvO with up-down separation using various values of sea-floor resistivity (Adapted from Roth, F., 2007).

Practically, in order to make the best choice of sea floor resistivity, ρ_{SF}, 1D-Inversion will be performed to find out the best background model with a sea floor resistivity (background resistivity) value as close as of reality.

1D-Inversion is a method of finding the best conductivity model explaining the real data. The resistivity of sea water, sea floor (top formation), intermediate formation and basement (half space) are needed as the input in order to create a synthetic model which the plots from it will be compared to the real data.

As a matter of fact, the algorithm of calculating the misfit between the real data and synthetic data is purely mathematical; hence the geological knowledge of the survey area is particularly important in inversion. Without the knowledge regarding the geology of the area, say the depth and the resistivity of the basement, any combinations of various resistivity values might create a so-called 'best model' with small error, which is invalid from geological point of view.

Figure 4.3 and Figure 4.4 show MvO and PvO plots of 2 synthetic models that created by different sets of conductivity parameters. Figure 4.3 plotted from a model which has a half space resistivity as high as 92.6 Ωm at the in-towing part; while the plot shown in Figure 4.4 is plotted from a model which has $7.0\,\Omega m$ at the in-towing part of the model. Note that both models give almost same plot compare to of real data.

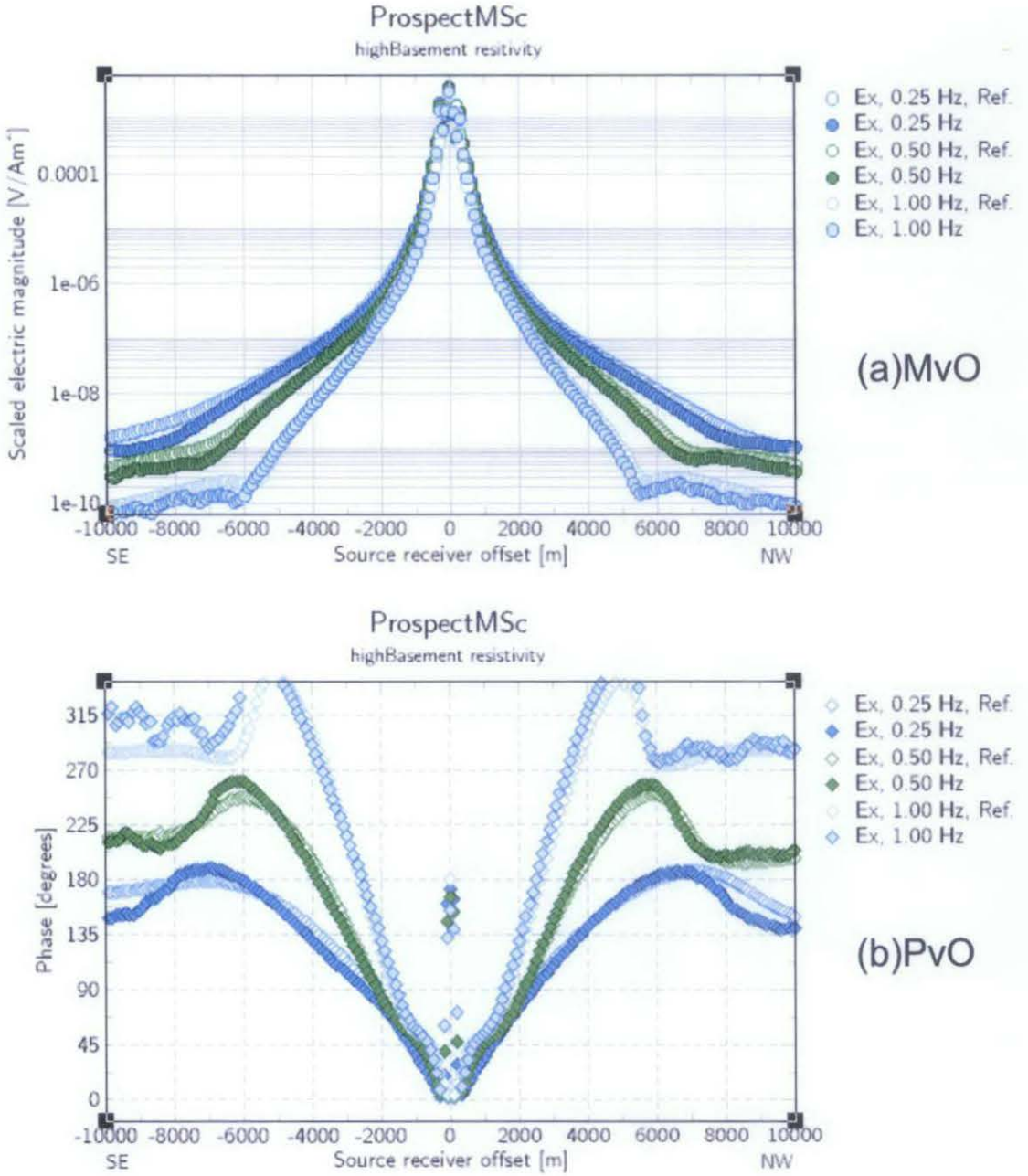

Figure 4.3: MvO and PvO plotted from a synthetic model with its resistivity parameters as follow: (in-towing part) $1.6\,\Omega m$ at top formation, $3.24\,\Omega m$ at intermediate formation, and $92.62\,\Omega m$ at half space; (out-towing) $1.6\,\Omega m$ at top formation, $3.36\,\Omega m$ at intermediate formation, and $9.66\,\Omega m$ at half space.

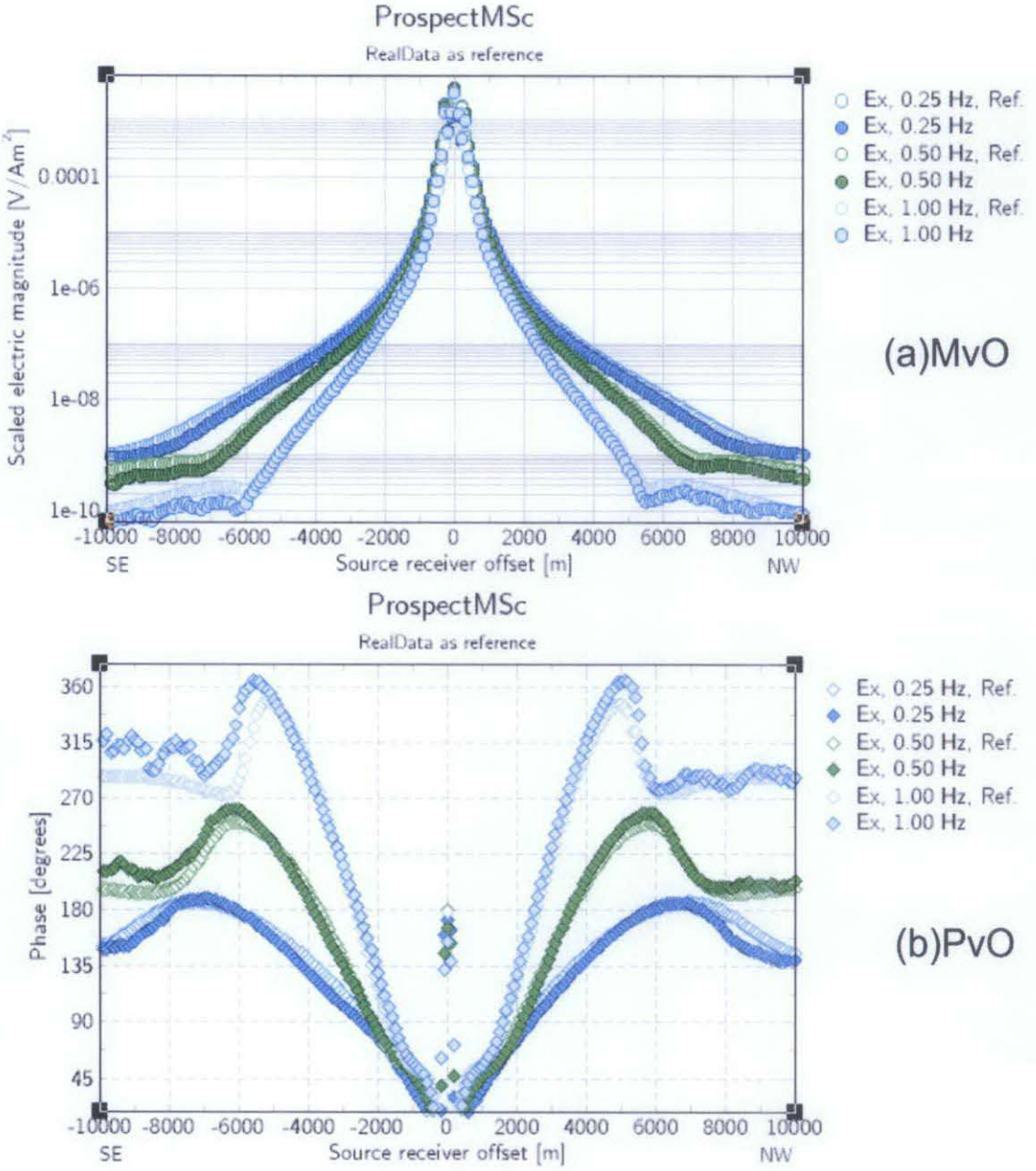

Figure 4.4: MvO and PvO plotted from a synthetic model with its resistivity parameters as follow: (in-towing part) $1.63\,\Omega m$ at top formation, $4.06\,\Omega m$ at intermediate formation, and $7.0\,\Omega m$ at half space; (out-towing) $1.52\,\Omega m$ at top formation, $3.98\,\Omega m$ at intermediate formation, and $7.0\,\Omega m$ at half space.

5. CHAPTER 5: PROSPECT INVESTIGATION

Data fusion or data integration is the main approach in order to study and understand a geological prospect. The optimization of SBL study will be only achieved with the information from seismic and the other exploration method like AVO analysis. Under this chapter, the study prospects will be examined using the data from 3D seismic, AVO analysis as well as SBL survey.

2360 km^2 of 3D seismic in Block 2F was shot in year 2002 and it provides data of high quality and high resolution compared to several 2D seismic lines that shot prior to it. The study of Block 2F by Theresia Heru Kuswardhany *et al.* 2006 was basically focusing on the 3D seismic coverage with the correlation from regional 2D seismic lines and total number of 66 nearby wells.

Amplitude versus offset, AVO, analysis is used to detect the seismic signal anomaly due to the contrast of seismic impedance and Poisson's ratio of the medium where the wave is traveling in. The amplitude of the anomaly is closely related to the source-receiver offset. The AVO analysis by Theresia Heru Kuswardhany *et al.* 2007 was a continuous study on the area which further zoomed in some perspectives prospects of the area, including Prospect A and Prospect B of our study. The study was fully conducted using Well-Seismic Fusion (WSF) software of Landmark. The result of AVO analysis is presented in several panels of CMP gathers with different NMO velocity. Apparently with a right NMO velocity applied, the changes of amplitude with offset can be easily seen after the NMO correction of the gathers.

5.1 Prospect A

5.1.1 3D seismic and AVO analysis

Prospect A has the biggest closure among the rest in Block 2F. However, the presence of shale diapir might have ruined the quality of the reservoir. Besides, shale diapir penetration creates masking effect on seismic section and makes better seismic interpretation almost impossible. Figure 5.1 shows a seismic section of Prospect A and Figure 5.2 is a seismic section that shows the shale diapir in Prospect A.

The results of the AVO analysis on this prospect was shown in CMP gathers as well as both near and far stack of the seismic data, illustrated in Figure 5.3. From the AVO analysis, we can obviously see that the high amplitude of seismic occur at the flank of the Prospect A's structure, but nothing prospective is observed at the crest of the structure.

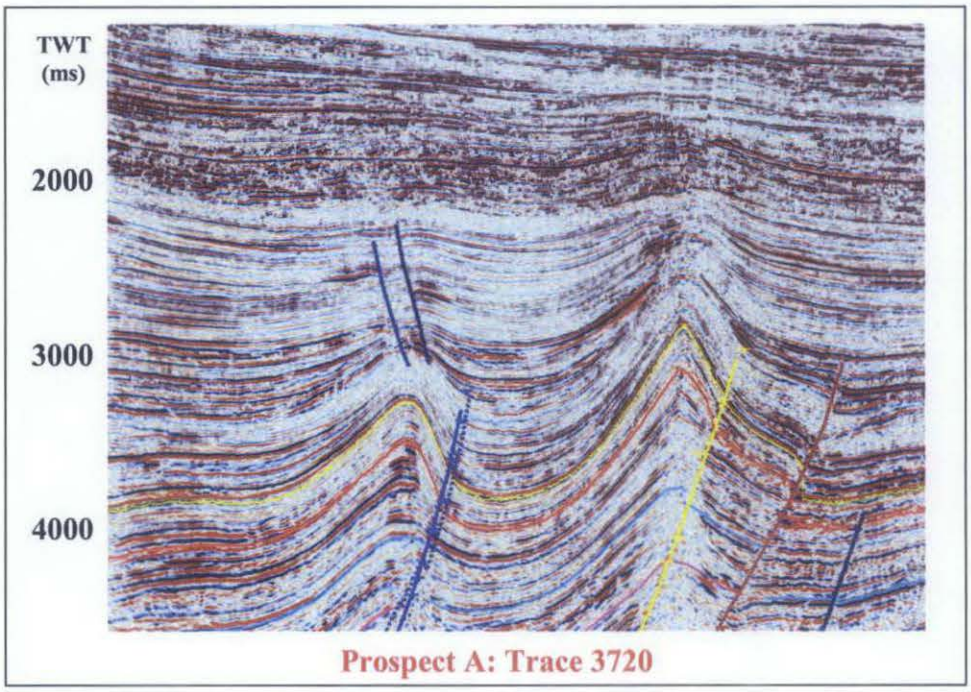

Figure 5.1: Full stack seismic section (Trace 3720) of Prospect A.

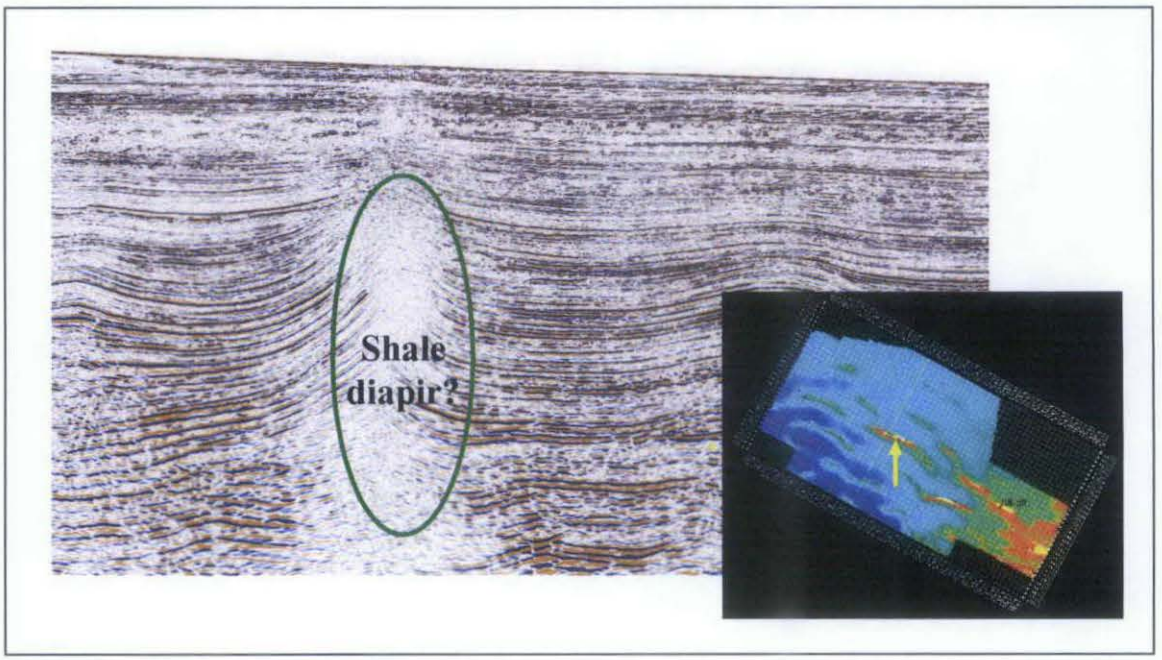

Figure 5.2: Shale diapir seen in one of the seismic trace crossing Prospect A. The shale diapir masks the seismic section and makes proper seismic interpretation almost impossible.

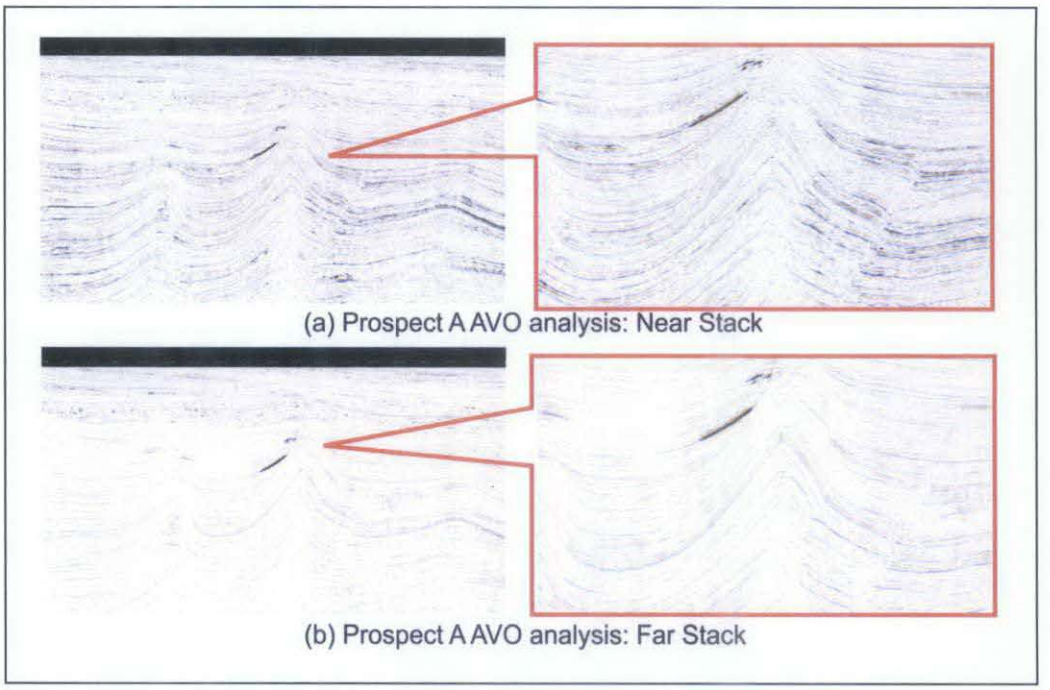

Figure 5.3: AVO analysis showing the difference between near stack and far stack of seismic (Trace 3720) of Prospect A. Pictures at the right panel are zoon-in of Prospect A. Note that a high amplitude anomaly detected at the flank of the structure in far stack section. There's no high amplitude anomaly at the crest of the structure.

5.1.2 SBL study

SeaBed Logging (SBL) survey performed over this prospect is a 2D survey line which aligned along the crest of the prospect as shown in Figure 5.4. 24 receivers had been deployed for the survey, and the 5th receiver and the 20th receiver sit at both sides of edge of the prospect. The towing direction is from Northwest to Southeastward, and the 21st receiver is chosen as reference receiver for Normalization plot, after taking into account the data quality and the navigation data of the receiver.

To preview the response of a prospect towards SBL method, a feasibility study is conducted prior to carrying out of the SBL survey. In the feasibility study, a 1D resistivity model is created by referring to the resistivity data from near by wells. The SBL response towards the 1D model will be then compared to the real response after survey.

Figure 5.5 illustrates the resistivity model of Prospect A which was created according to the resistivity data obtained from a near-by well located 29.4 km south-west of Prospect A, as well as the expected SBL response towards the model.

Figure 5.6 shows three summary plots of Prospect A at near, intermediate and far offset, respectively after the survey has been conducted. Note that the real response of Prospect A is close to the response acquired by the resistivity model in feasibility study.

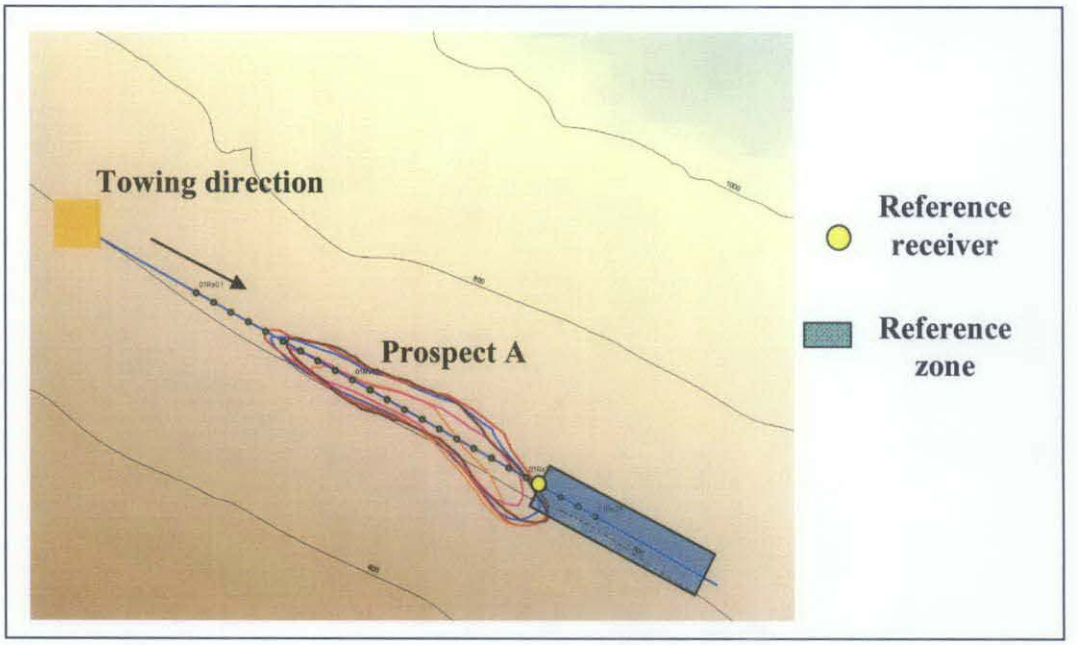

Figure 5.4: SBL survey line on Prospect A. The 21st Receiver is chosen to be the reference receiver after considering its data quality and navigation data.

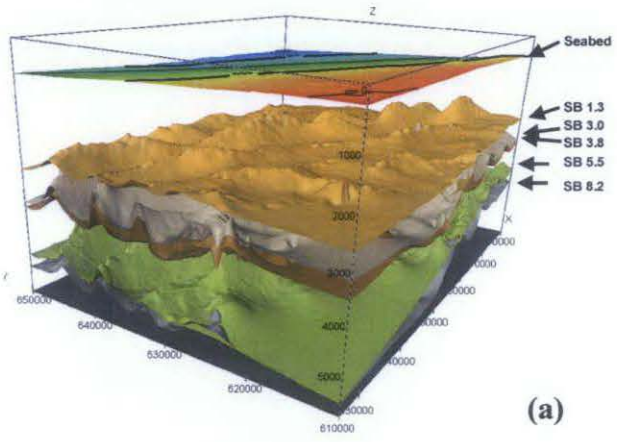

(a)

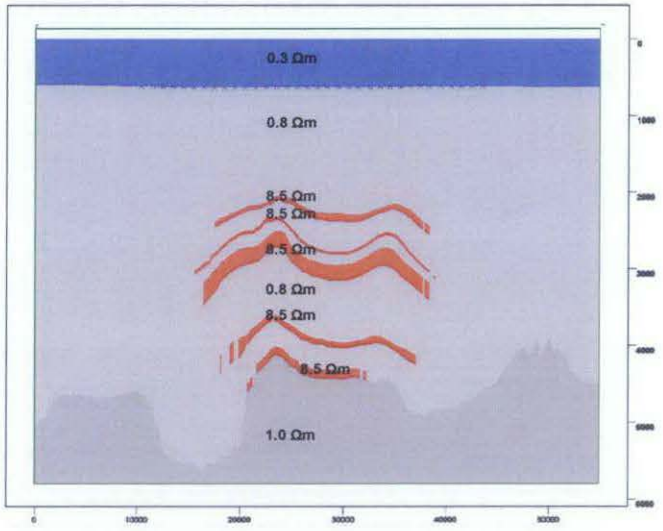

(b)

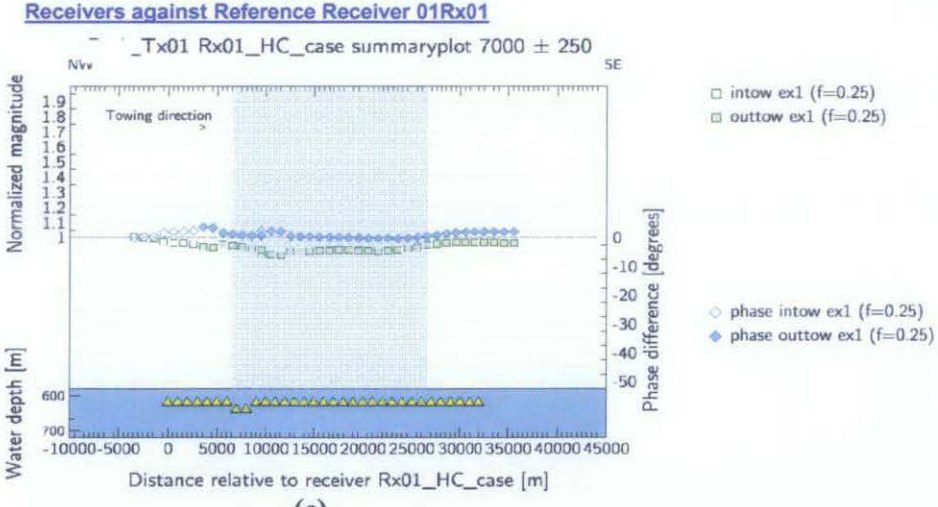

(c)

Figure 5.5: (a) 3D overview of Prospect A; (b) Numerical model of Prospect A, showing the resistivity values for each reservoir; (c) show summary plots of NMVO and PDVO against reference receiver at far source-receiver offset (7000 ± 250 m).

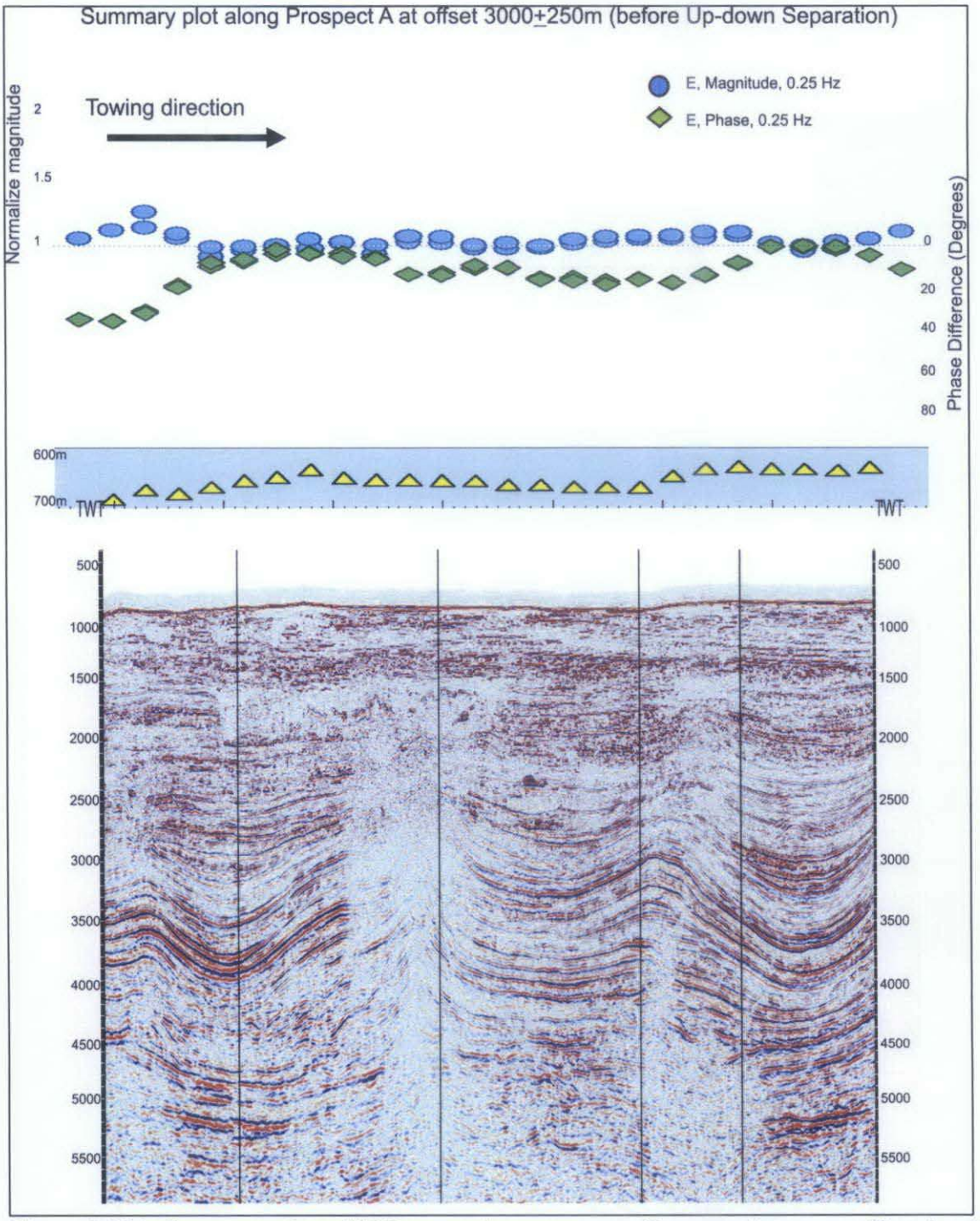

Figure 5.6(a): Summary plot of SBL anomaly response on Prospect A at near offset, i.e. 3000 ± 250 m. Note that there's no clear anomaly seen in the plot.

13.7 25.6 0.535156

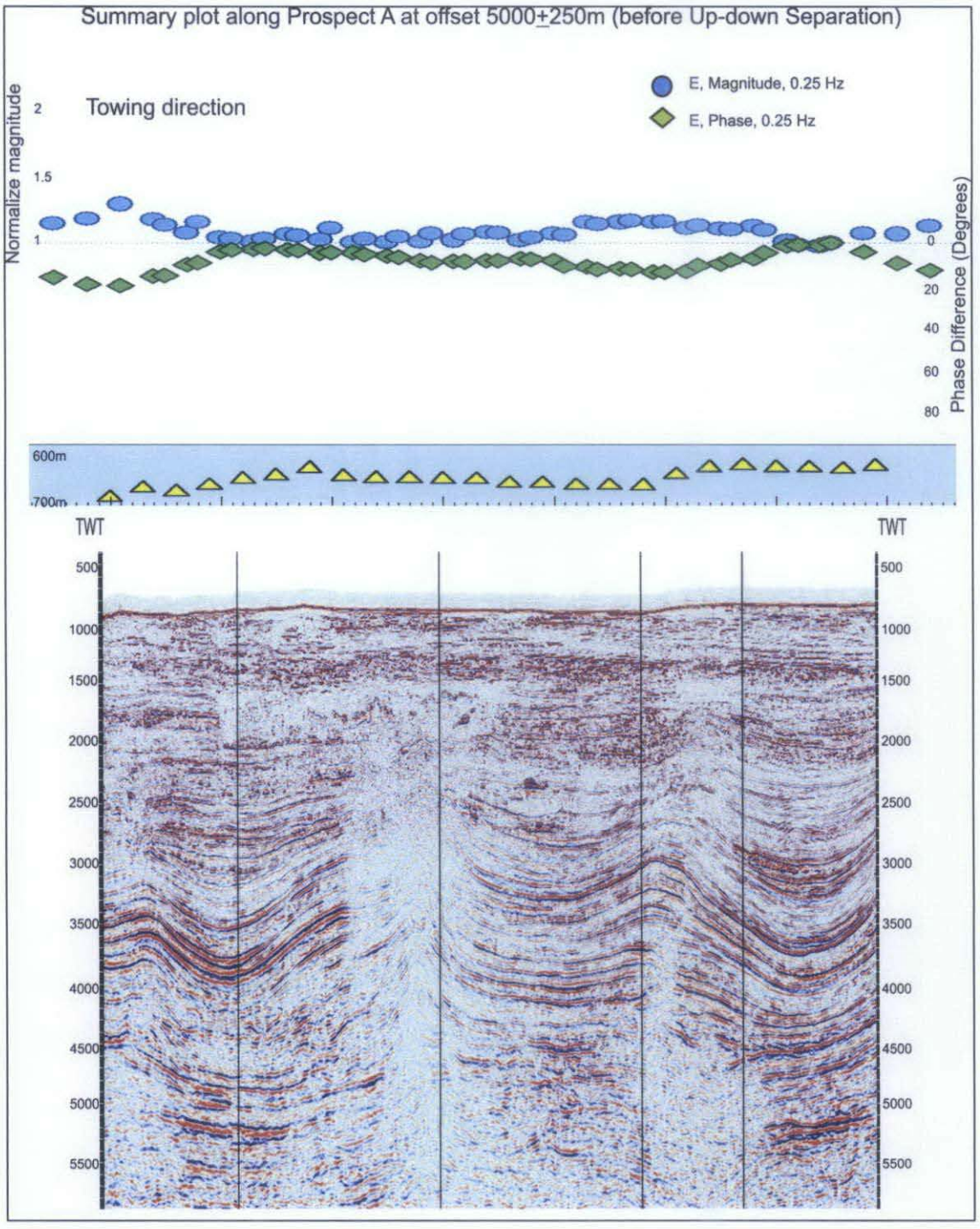

Figure 5.6(b): Summary plot of SBL anomaly response on Prospect A at intermediate offset, i.e. 5000 $\pm$ 250 m. A weak resistivity anomaly has been detected at the location of 15th receiver to 20th receiver.

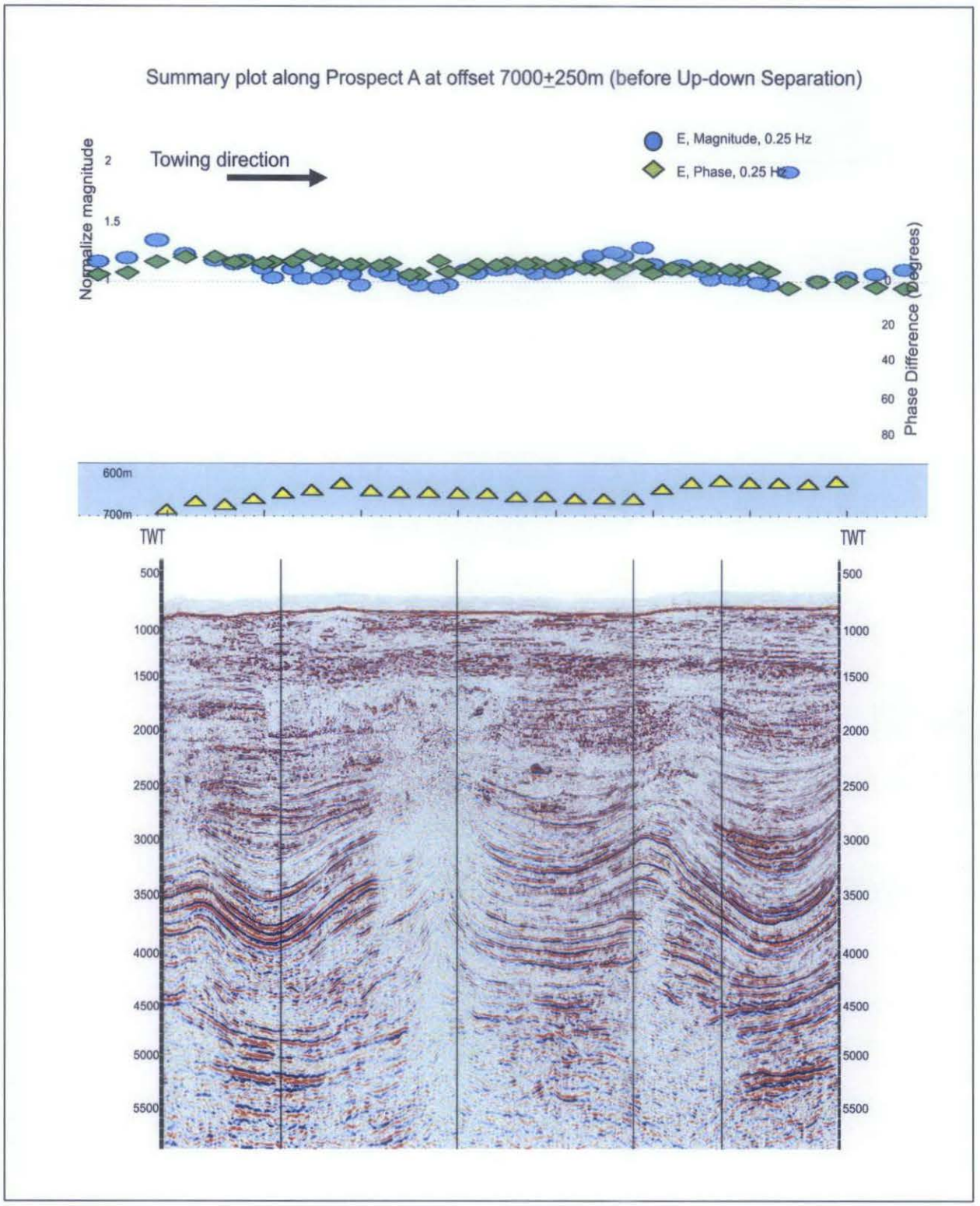

Figure 5.6(c): Summary plot of SBL anomaly response on Prospect A at far offset, i.e. 7000 ± 250 m. Note that the plot started to get scattered as the result of noise and bathymetry interference at far offset.

While the summary plots of Prospect A displayed above show a rather weak anomaly response and, as the matter of fact that the water depth of the prospect is rather shallow, there's the possibilities of airwave masking the anomaly response. Hence, separation of up-going and down-going wave via up-down separation method is performed on its SBL data.

To perform up-down separation, background resistivity or top formation resistivity needs to be known before hand. By running 1D inversion, the best 'possible' top formation resistivity can be figured out, although there are another few factors like half space resistivity, intermediate formation resistivity and depth of formations could influence the matching of the so-called best-fit curve to of real data.

In the case of Prospect A, the top formation resistivity used for up-down separation is $1.55\,\Omega m$, and as the result after up-down separation, it's obvious that the airwave effect has been toned-down as the phase difference is obviously lower than of before up-down separation. Despite of the steps that are used to analyze air wave condition of the survey, a hint regarding the airwave level that get be obtained from a summary plot is that, the lower the phase difference is, the less airwave effect the data has. This can especially be seen in the intermediate offset summary plot in Figure 5.7(b) and far offset summary plot in Figure 5.7(c).

However, in term of boosting the anomaly response of the plot, up-down separation doesn't seem to be achieving the objective. There's only a slight increase of normalize magnitude in intermediate offset plot (Figure 5.7(b)) and far offset plot (Figure 5.7(c)).
Anyway, the slight increase doesn't bear any significant meaning in proving the existence of any high resistivity bodies lie underneath.

By referring the case back to what shown in 3D seismic and AVO analysis, there's an apparent explanation that accounts for the weak anomaly response happens in the plot after up-down separation. From the seismic interpretation and AVO analysis, we knew that there's neither clear DHI nor Class III AVO response in the crest of Prospect A and SBL study showed that there's lack of high resistivity bodies lay along the crest of Prospect A. Both physical properties i.e. acoustic impedance and resistivity of possible HC are not detected along the

crest. Both measurements pointed to a same result, which is a 'negative' for the existence of HC. In another word, SBL method in this case is compatible to the seismic and AVO analysis.

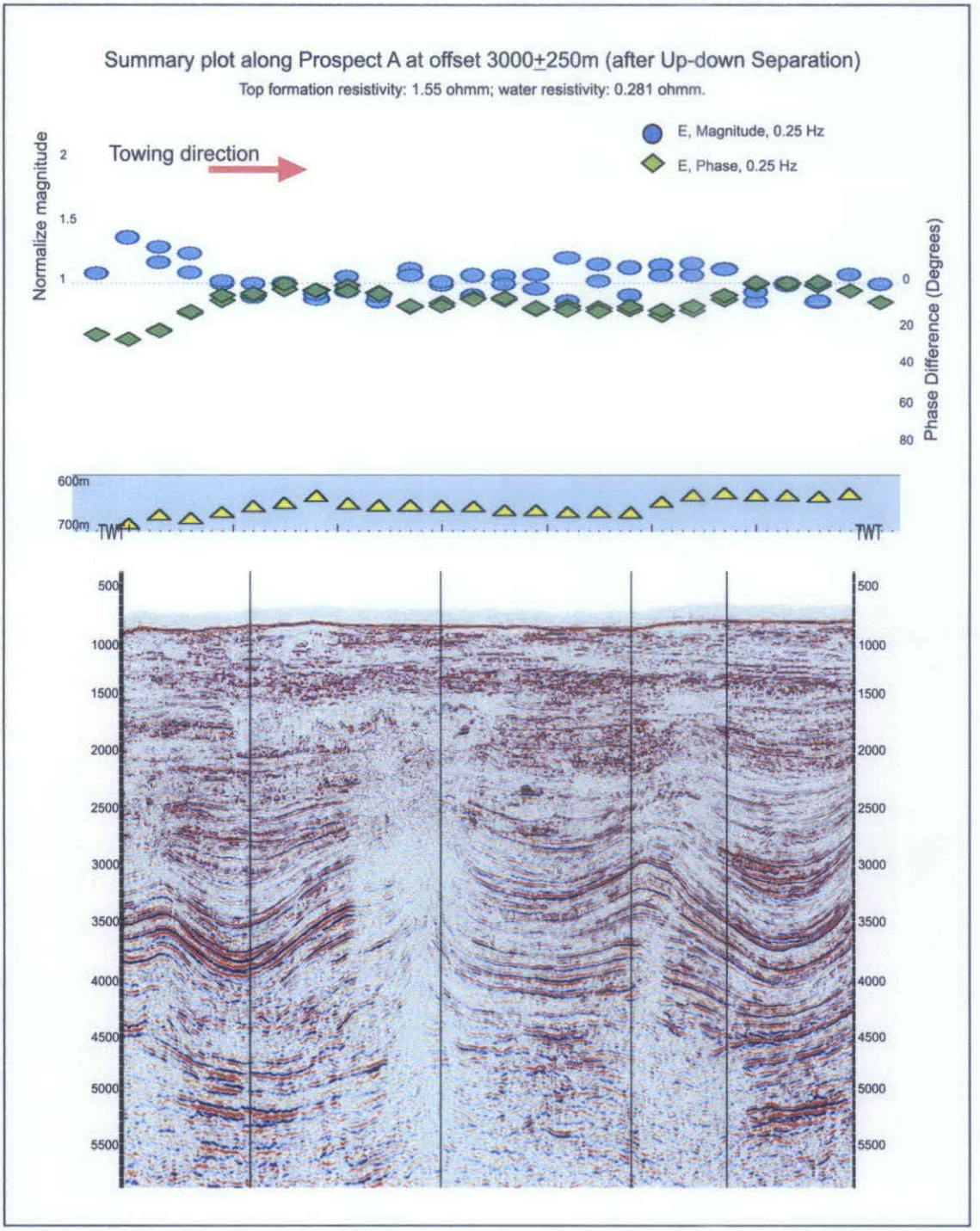

Figure 5.7(a): Summary plot of SBL anomaly response on Prospect A at near offset, i.e. 3000 $\pm$ 250 m, after up-down separation with 1.55 Ωm top formation resistivity.

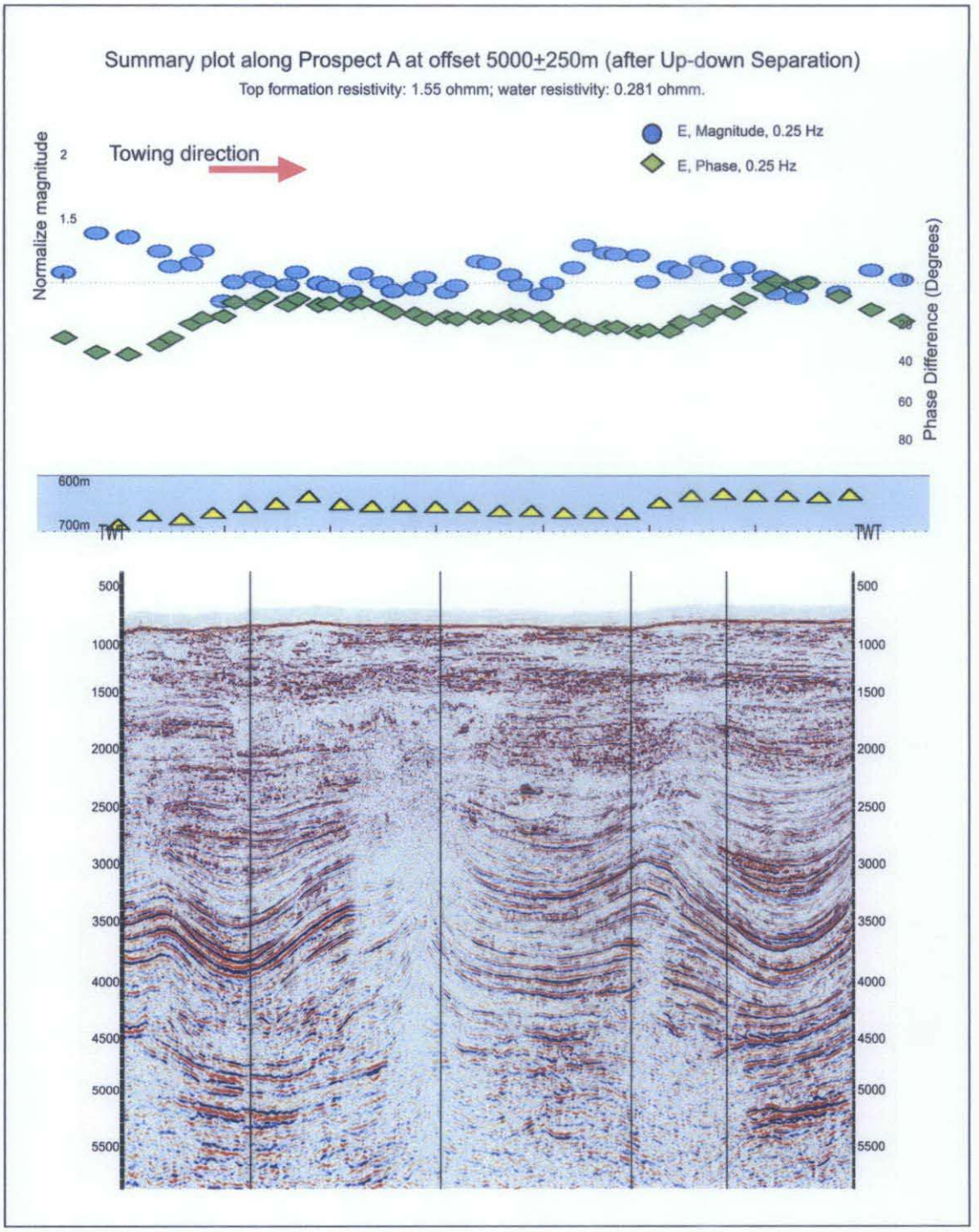

Figure 5.7(b): Summary plot of SBL anomaly response on Prospect A at intermediate offset, i.e. 5000 $\pm$ 250 m, after up-down separation with 1.55 Ωm top formation resistivity. Note that there's a slight increase in normalized magnitude compared to the plot before up-down separation. The airwave effect is eliminated as the phase difference increased after up-down separation.

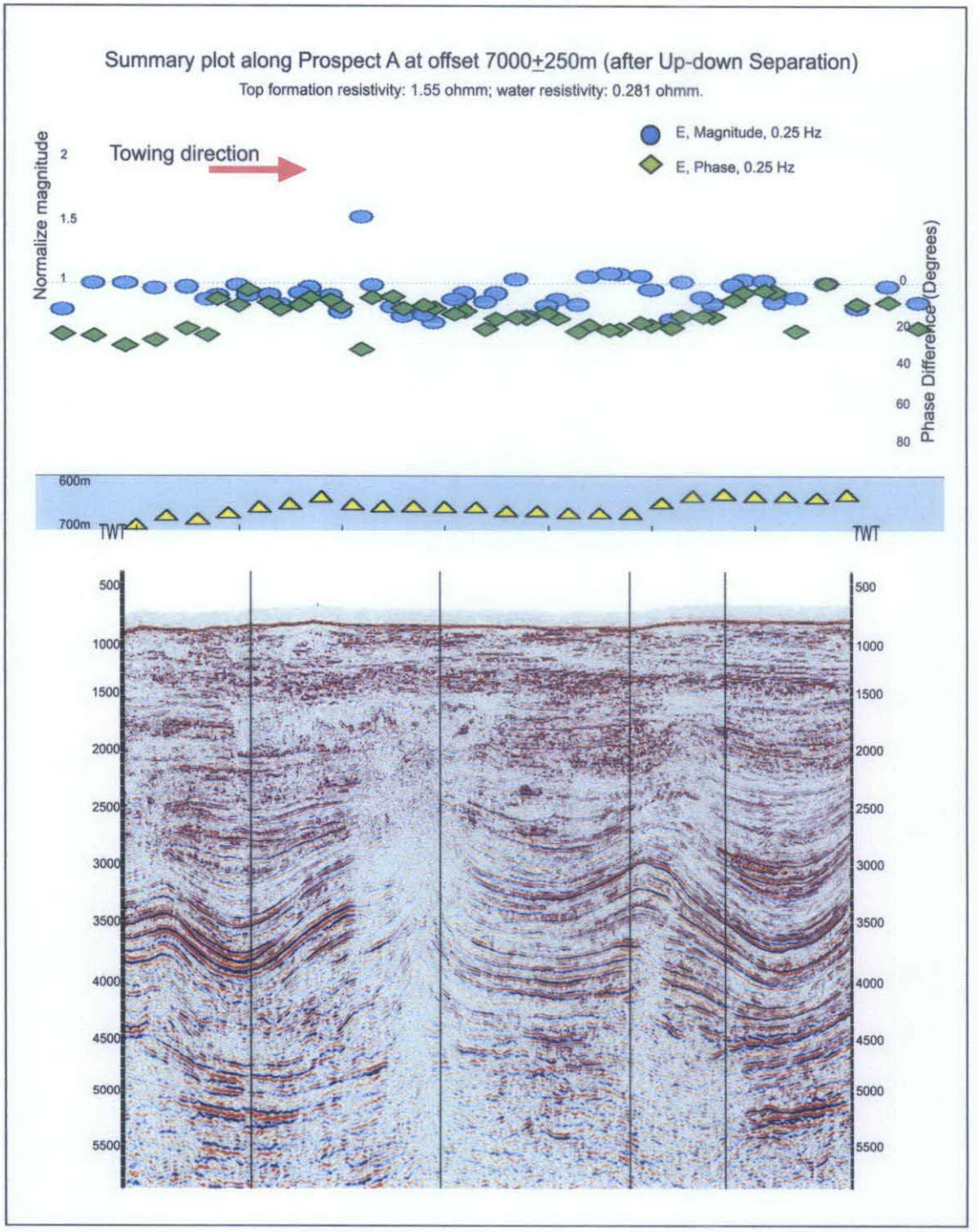

Figure 5.7(c): Summary plot of SBL anomaly response on Prospect A at intermediate offset, i.e. 7000 $\pm$ 250 m, after up-down separation with 1.55 Ωm top formation resistivity. Note that the airwave effect is eliminated as the phase difference increased after up-down separation.

5.2 Prospect B

5.2.1 3D seismic and AVO analysis

Prospect B features anomalies of strong amplitude in seismic section. As shown in Figure 5.8, the possible pull-down effect is obviously seen (in red circle) and it is a characterization of a possible gas cap on top of it (in blue square 1). Besides, there are high amplitude anomalies observed at the flank of the crest. The AVO analysis aimed at anomalies that observed at both the crest and the flank of the structure. Figure 5.9 and Figure 5.10 illustrate the results of AVO analysis on anomaly 1 and anomaly 2 of the seismic section. The amplitude of seismic signal on CMP gathers for both AVO analyses increase with offset. They are Class III AVO response which indicates existence of gas.

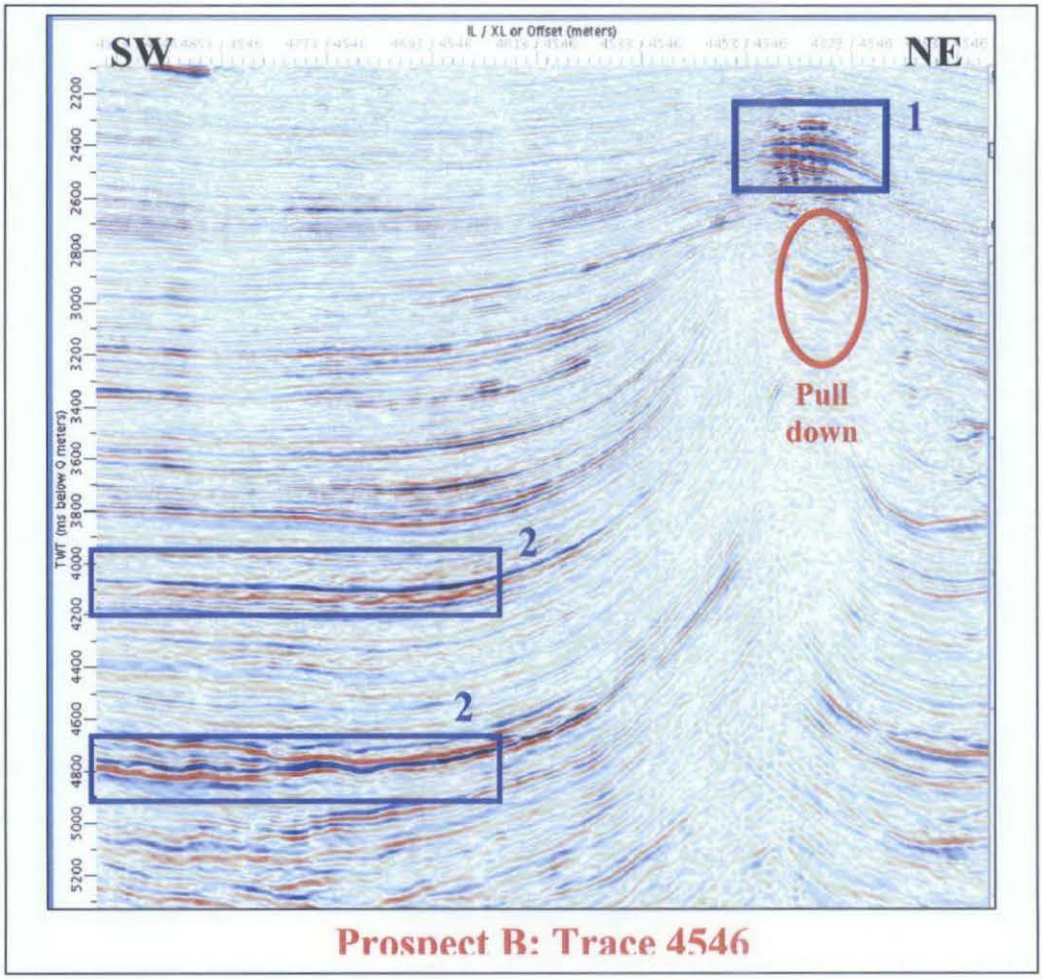

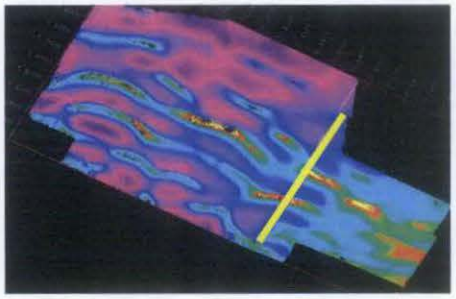

Figure 5.8: Seismic section across Prospect B. Red circle points out the pull-down effect of seismic signal that might be caused by the gas cap on top of it. Blue squares show the bright spots at the crest and the flank of the structure. The inset down left shows the location of the seismic section.

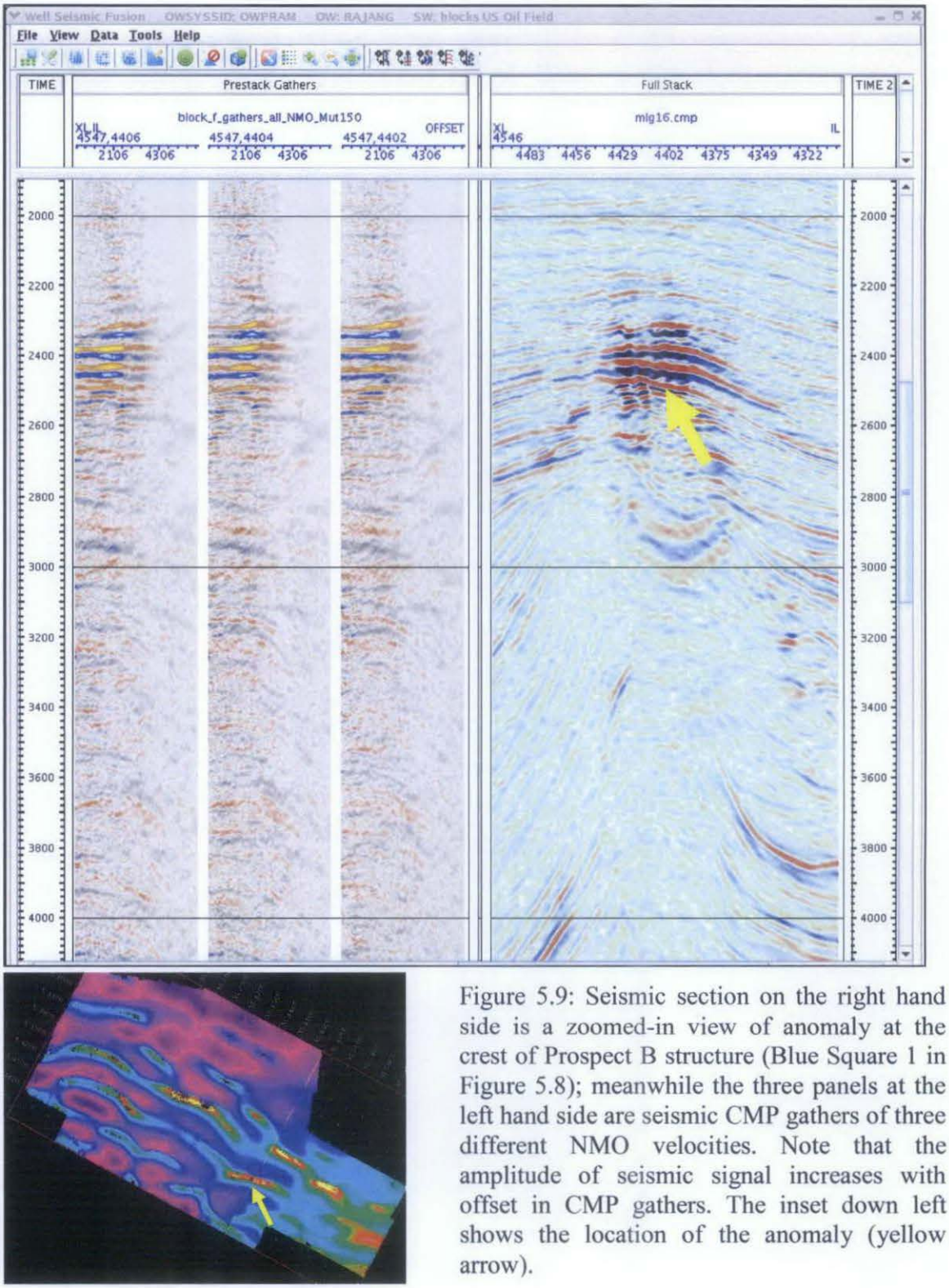

Figure 5.9: Seismic section on the right hand side is a zoomed-in view of anomaly at the crest of Prospect B structure (Blue Square 1 in Figure 5.8); meanwhile the three panels at the left hand side are seismic CMP gathers of three different NMO velocities. Note that the amplitude of seismic signal increases with offset in CMP gathers. The inset down left shows the location of the anomaly (yellow arrow).

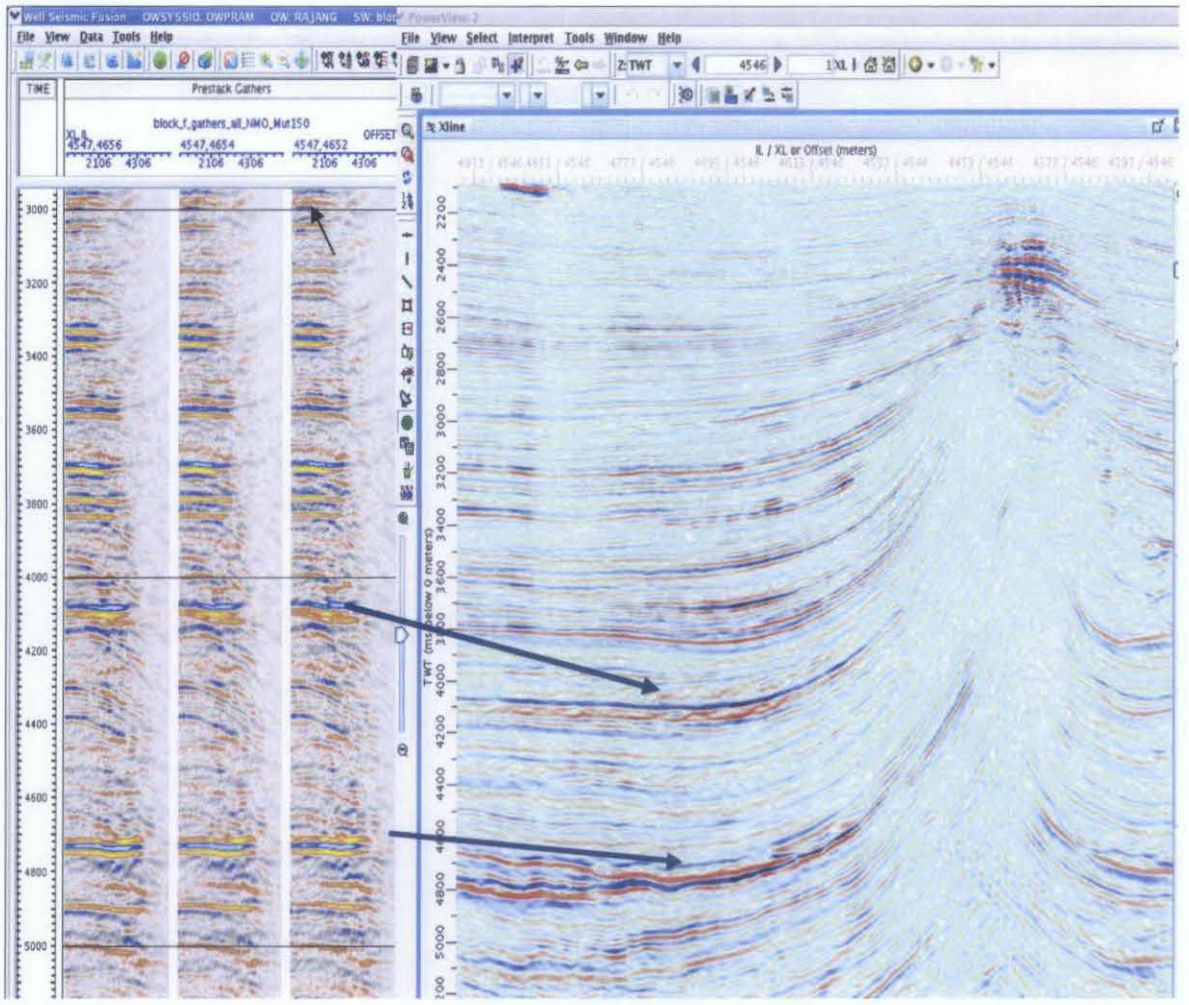

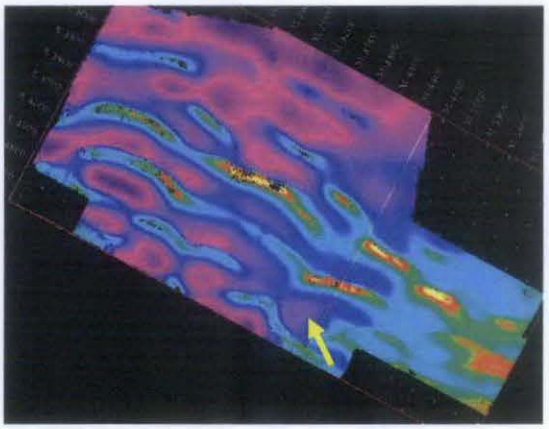

Figure 5.10: Seismic section on the right hand side is a zoomed-in view of anomalies at the flank of Prospect B structure (Blue Square 2 in Figure 5.8); meanwhile the three panels at the left hand side are seismic CMP gathers of three different NMO velocities. Note that the amplitude of seismic signal increases with offset in CMP gathers. The inset down left shows the location of the anomaly (yellow arrow).

5.2.2 SBL study

The SBL study over Prospect B, despite the amplitude anomalies at the flank of the structure, only spread-out along the crest of Prospect B. 19 receivers had been deployed and the 5th to the 15th receiver are the ones sit right on top of the prospect as shown in Figure 5.11. The towing direction of the survey is from Northwest to Southeastward.

Figure 5.12 shows the result of feasibility study over Prospect B. The resistivity model of Prospect B is created according to a near-by well that is located 13.5 km north-west of Prospect B. The SBL response towards the model is very positive as seen in Figure 5.12(c) .

Figure 5.13 shows three summary plots of Prospect B at near, intermediate and far offset, respectively, with no up-down separation performed on the data. In plotting these summary plots, the 1st receiver is used as the reference receiver as it collects data outside of the prospective zone i.e. background resistivity, and the consideration of its data quality and navigation information also have been taken into account.

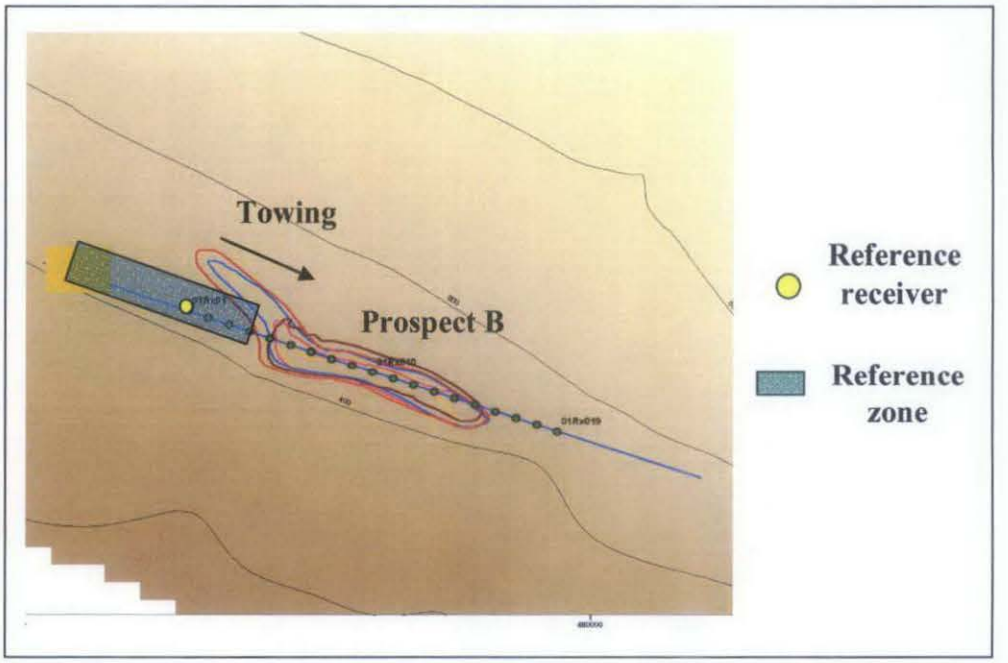

Figure 5.11: SBL survey line on Prospect B. 19 receivers had been deployed for this survey and the 5th receivers and the 15th receivers bounded both edges of the prospect. The 1st Receiver is chosen to be the reference receiver after considering its data quality and navigation data.

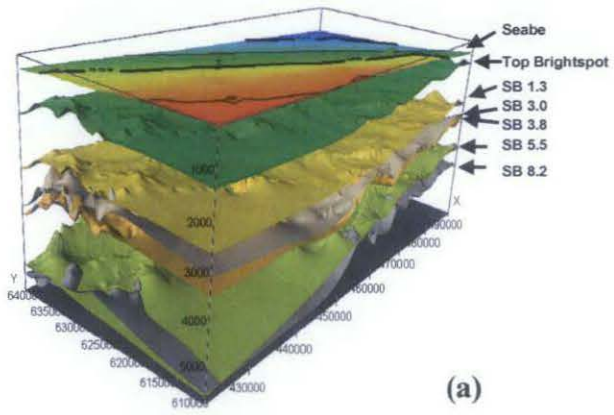

(a)

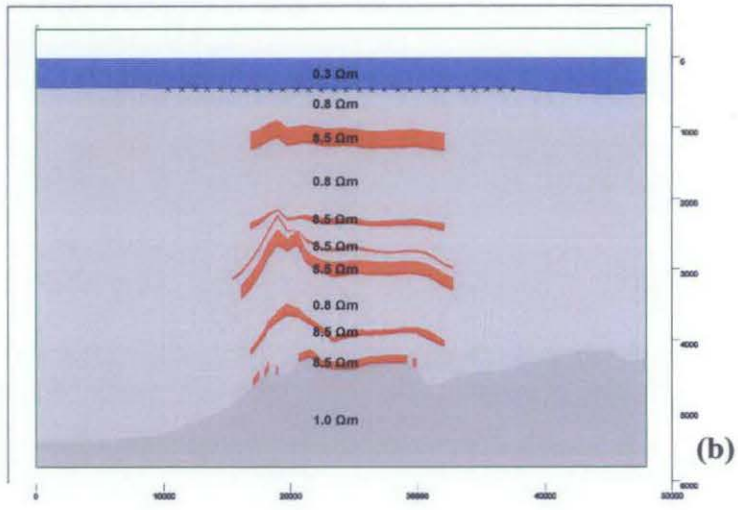

(b)

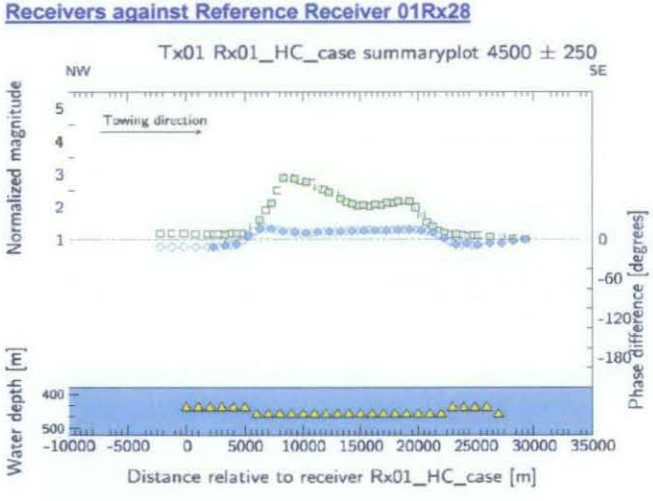

(c)

Figure 5.12: (a) 3D overview of Prospect B; (b) Numerical model of Prospect B, showing the resistivity values for each reservoir; (c) shows summary plots of NMVO and PDVO against reference receiver.

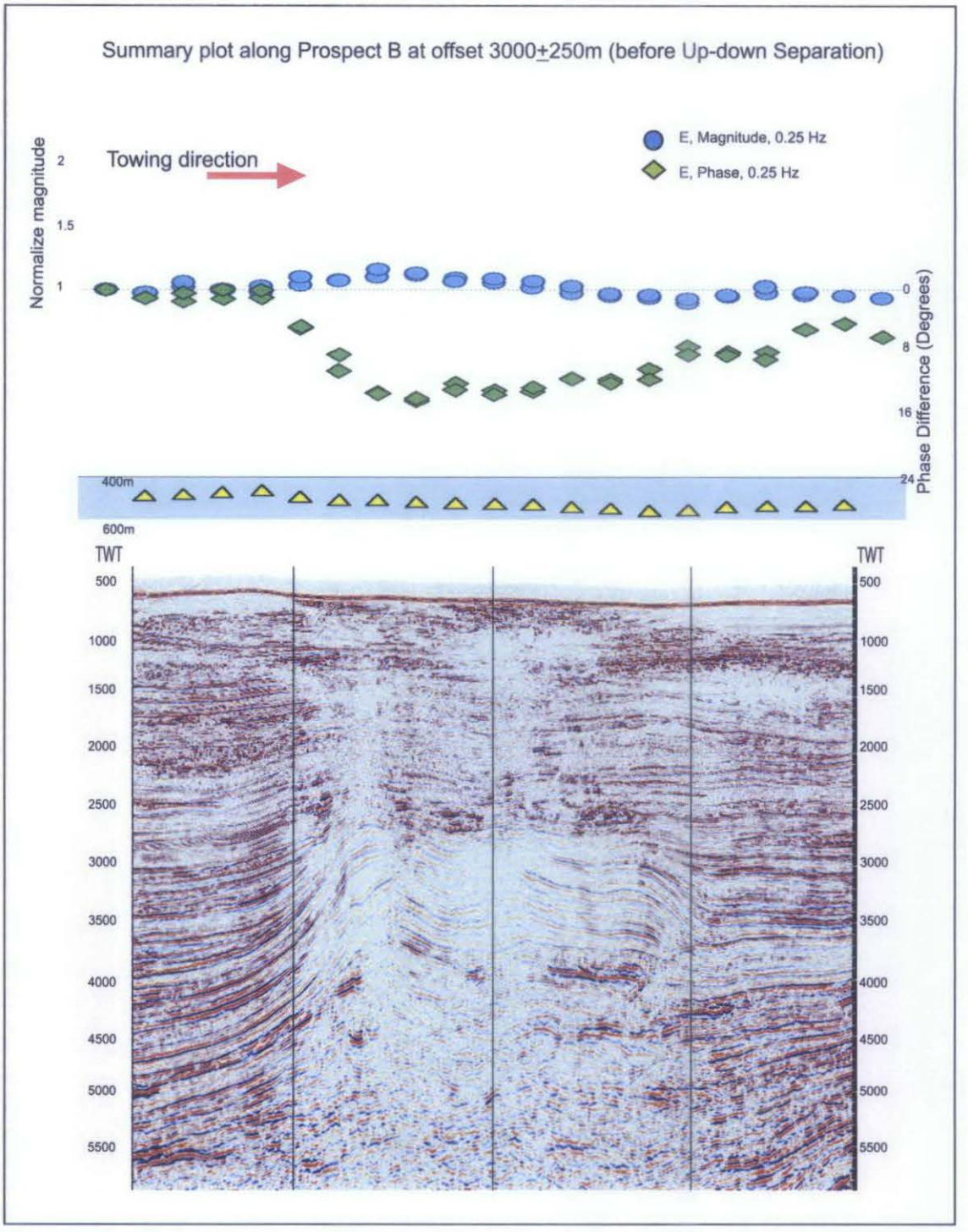

Figure 5.13(a): Summary plot of SBL anomaly response on Prospect B at near offset, i.e. 3000 ± 250 m. Note that there's only slight response of resistivity anomaly recorded.

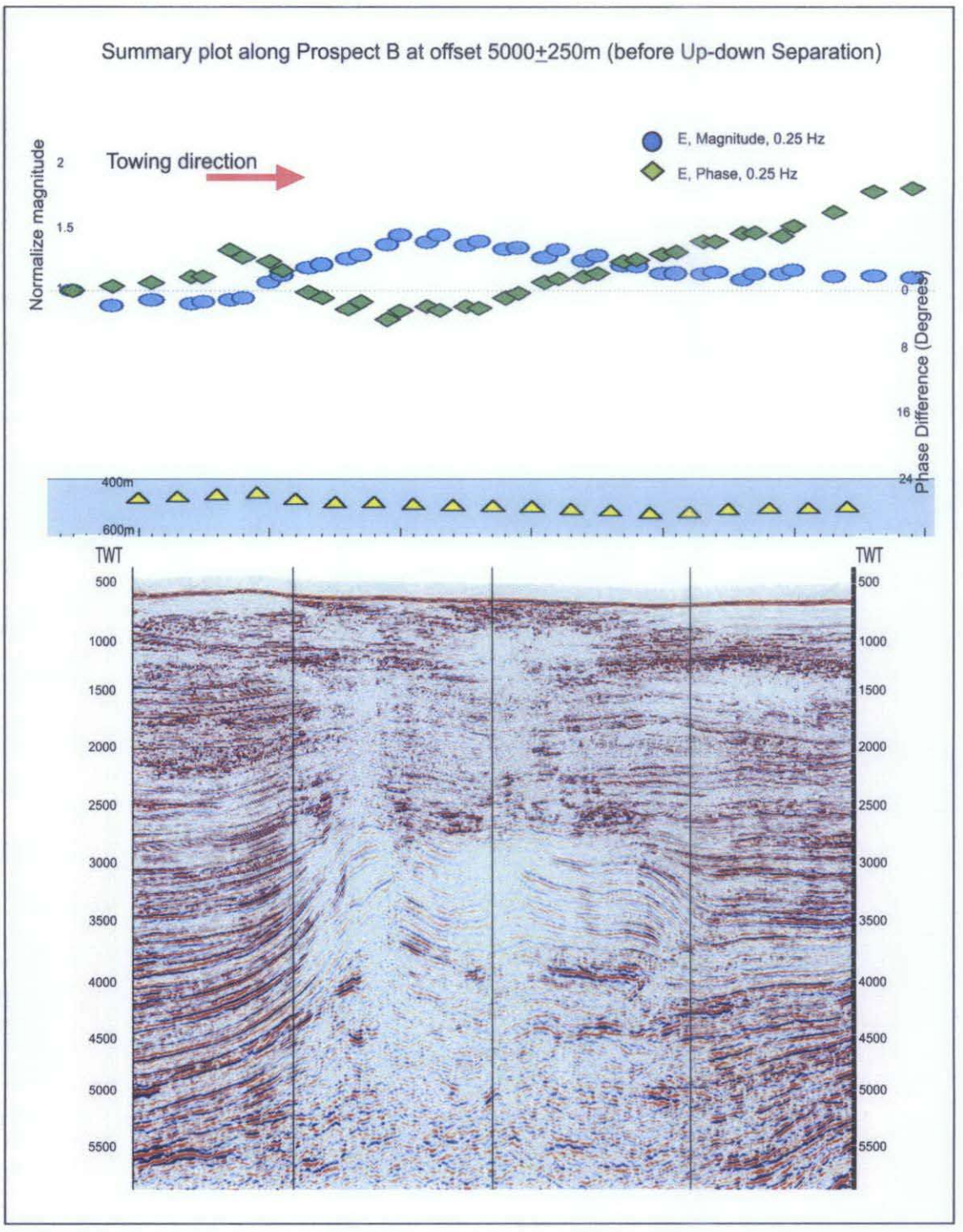

Figure 5.13(b): Summary plot of SBL anomaly response on Prospect B at intermediate offset, i.e. 5000 $\pm$ 250 m. Data of good quality acquired and it shows there's resistivity response occurred within the range between the 5th receiver to the 15th receiver, which is the location of prospective area of Prospect B.

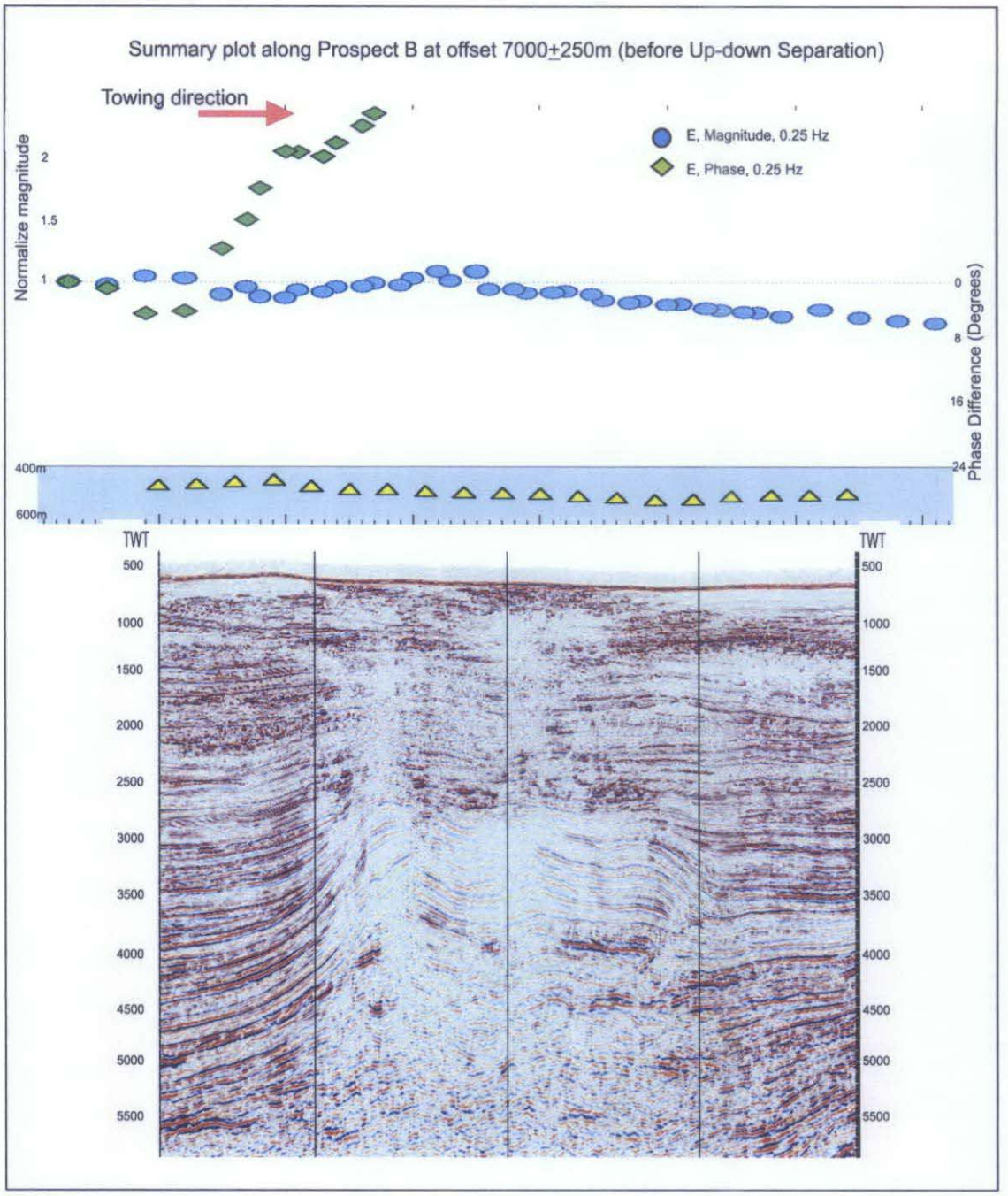

Figure 5.13(c): Summary plot of SBL anomaly response on Prospect B at far offset, i.e. 7000 ± 250 m. Note that the high build up of phase data might be due to the tremendous airwave effect occurred at far offset.

Airwave effect is expected in Prospect B as the water depth of Prospect B is shallower compare to Prospect A. Hence, up-down separation is necessary to boost the anomaly response that comes from up-going wave component.

To perform up-down separation, background resistivity or top formation resistivity needs to be known before hand. By running 1D inversion, the best 'possible' top formation resistivity can be figured out, although there are another few factors like half space resistivity, intermediate formation resistivity and depth of formations could influence the matching of the so-called best-fit curve to of real data.

In the case of Prospect B, the top formation resistivity used for up-down separation is $1.23\,\Omega m$, and as the result after up-down separation, it's obvious that the airwave effect has been toned-down as the phase difference is obviously lower than of before up-down separation. Despite of the steps that are used to analyze air wave condition of the survey, a hint regarding the airwave level that get be obtained from a summary plot is that, the lower the phase difference is, the less airwave effect the data has. This can be noticed from the comparison between plots in Figure 5.13 and Figure 5.14.

Besides the subsidence of airwave effect's level, the anomaly responses show increment as well. A slight boost of anomaly response detected by the 5^{th} to the 9^{th} receiver at near offset in Figure 5.14(a) could be caused by the gas charge at shallow depth, around 1000 ms TWT. This shows that SBL would response only to any resistivity contrast down there but it won't promise the existence of a reservoir.

However, a stronger SBL anomaly response that is observed at intermediate offset might lead to an existence of a possible gas cap around 2000 ms – 2500 ms TWT, as displayed in Figure 5.14(b). The cross section of the gas cap is shown in Figure 5.8 while the AVO analysis of the possible gas cap is already shown in Figure 5.9. The result of both SBL study and AVO analysis tie well with the DHI showed in seismic in this case.

The result of up-down separation is obvious at far offset plot as seen from the comparison between Figure 5.13(c) and Figure 5.14(c) in term of lowering the air wave effect. Meanwhile, build-up on normalize magnitude plot in Figure 5.14(c) shows that there might be a resistivity anomaly detected at a deeper depth. It might be caused by the anomaly at 4000 ms TWT on seismic, which is interpreted as high pore pressured formation. Nevertheless, there are also possibilities of far offset noise which causes the SBL response.

SBL study over Prospect B is a case where we can show how SBL complementing AVO and seismic as these three methods tell a same story about the existence of possible HC accumulation at intermediate depth. However, there are also some confusions happened especially at far offset, where resistivity anomaly has been detected in SBL but only change of lithology property can explain from seismic instead of HC occurrence.

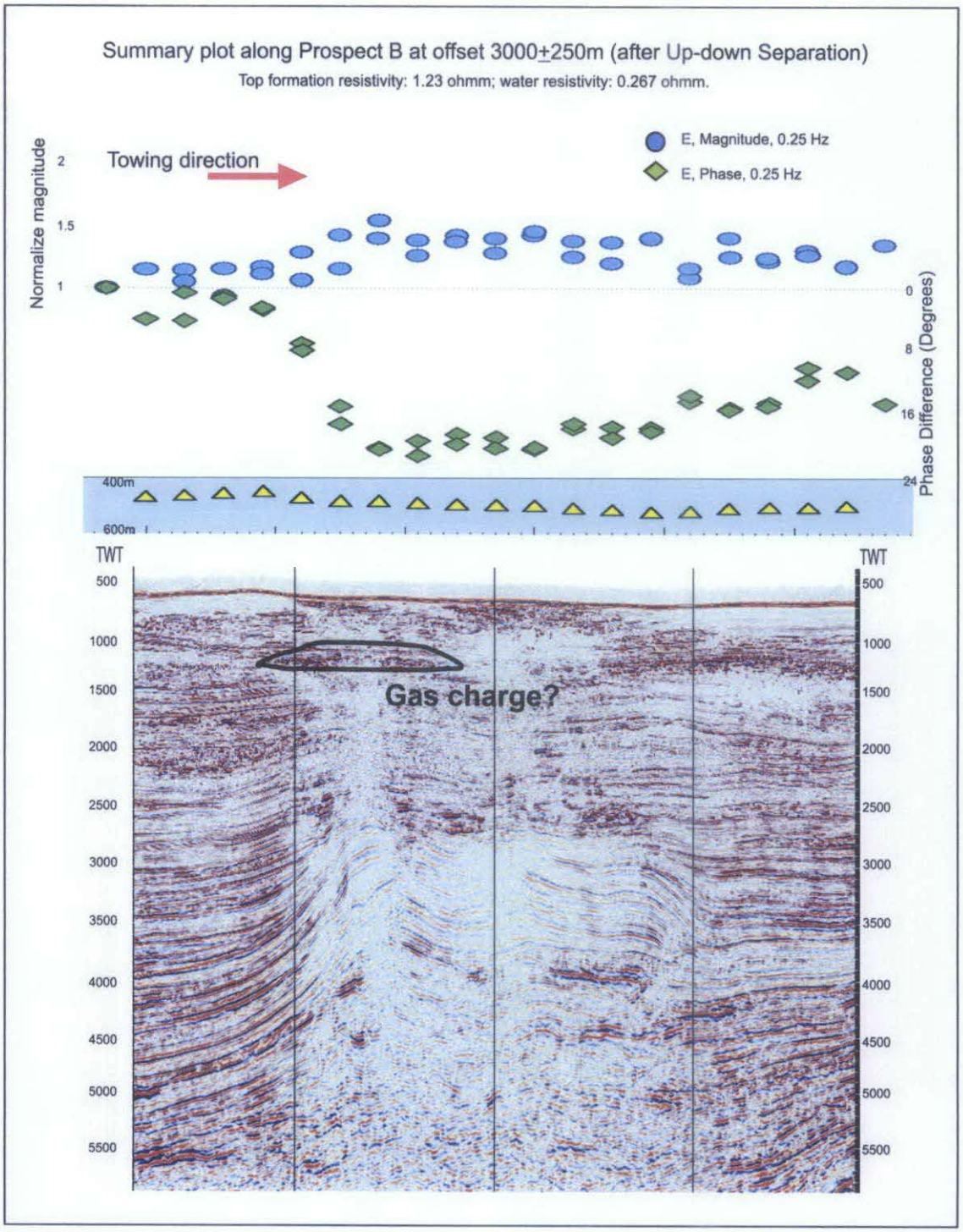

Figure 5.14(a): Summary plot of SBL anomaly response on Prospect B at near offset, i.e. 3000 ± 250 m, after up-down separation with 1.23 Ωm top formation resistivity. Note that the airwave effect is eliminated as the phase difference increased after up-down separation.

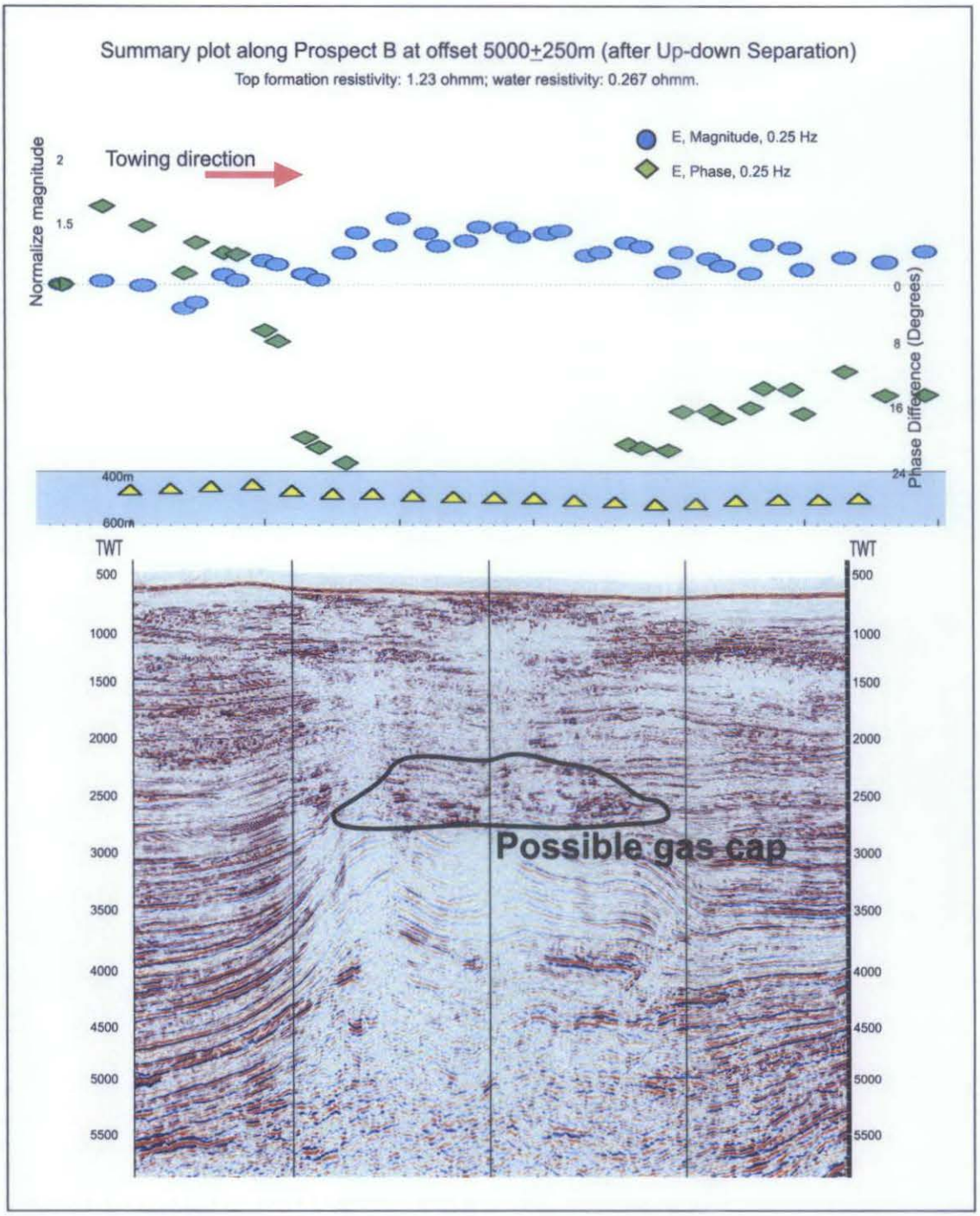

Figure 5.14(b): Summary plot of SBL anomaly response on Prospect B at intermediate offset, i.e. 5000 $\pm$ 250 m, after up-down separation with 1.23 Ωm top formation resistivity. The strong SBL response might probably due to the possible gas cap at 2000 ms to 2500 ms TWT on seismic section.

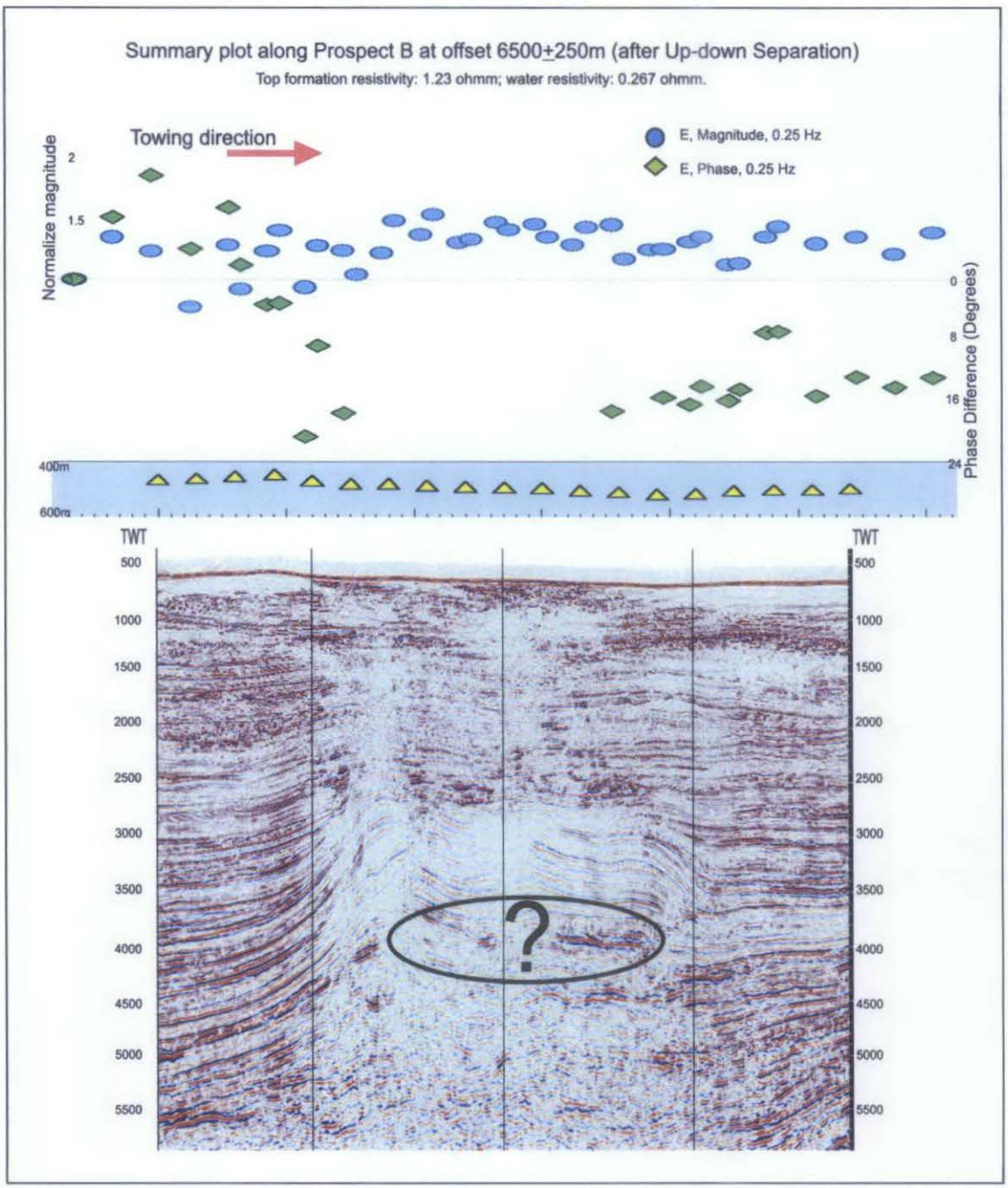

Figure 5.14(c): Summary plot of SBL anomaly response on Prospect B at far offset, i.e. 6500 ± 250 m, after up-down separation with 1.23 Ωm top formation resistivity. The anomaly response in SBL might be due to the anomaly happens at 3500ms – 4000 ms TWT on seismic, and might also be caused by far offset noise of SBL data.

6. CHAPTER 6: DISCUSSION AND CONCLUSION

SeaBed Logging (SBL) technology is not yet a stand-alone exploration method that can eliminate the uncertainties entirely in order to enhance the confidence level in exploration task. However, the technology is definitely gaining its importance due to its contribution in an era where data integration is so important in oil and gas exploration.

An undeniable advantage of SBL technology is the application of resistivity contrast in detecting the HC lies beneath. It's an independent physical property that allows us to further confirm the existence of HC, or vice versa, besides referring to the acoustic impedance anomaly in seismic and AVO analysis.

Nevertheless, SBL still has a lot of rooms for improvement. From the case study of Prospect A we realize that only inline data which is transmitted and received along the survey line bears meaningful significant for SBL responses. The broadside data, on the other hand, is wasted because it does not help in detecting the anomaly laterally, i.e. from both sides of the survey line.

The detection depth that derived from the source-receiver offset is merely estimation and the information is not much useful to develop a detailed geological study over the prospect. Advanced imaging method which includes CMP Inversion and Depth Migration is used to address the concern. It's always a next-step for SBL study in order to delineate geology property of a potential prospect.

A positive SBL response might be derived from an accumulated response from different resistive bodies that lie underneath. This is a risk that will be misguiding if the geology of the prospect area is not known. A positive magnitude build-up of SBL response from Prospect B can be due to a gas-prone reservoir, or several thin bedded gas-bearing siltstones, or maybe just a gas-charged formation which does not bring any value.

Besides, there are some uncertainties regarding the effect of water depth towards the SBL response. The survey over both Prospect A and Prospect B do not show relatively high magnitude compare to other shallower water depth surveys that had been carried out. While other factors such as low contrast of resistivity, bathymetry problem, relatively thin/small resistive body, etc., would have caused this low magnitude response, the suppression of response by the factor of deep water depth might be as critical and might need to be taken into consideration too. Techniques like Up-down Separation and newly-developed Surface Related Multiple Elimination (SRME) would probably be helpful in enhancing the resistivity response, but the efficiency of an SBL response in showing the true resistivity contrast quantitatively remains under-developed.

All and all, it's still the geology of the area that should be honored. The technology of exploration methods are tools that help us to obtain a better idea of what lies beneath, but the geology is still the eventual picture that to evaluate the efficiency of the tools.

REFERENCE

Amundsen, L., Løseth, L., Mittet, R., Ellingsurd, S., and Ursin, B. [2006] Decomposition of electromagnetic fields into upgoing and downgoing components. *Geophysics*, **71**, 211-223.

Chopra, S., Strack, K., Esmersoy, C., and Allegar, N. [2007] Introduction to CSEM. *The Leading Edge*, **26**(March), 323-325.

Eidesmo, T., Ellingsrud, S., MacGregor, L. M., Constable, S., Sinha, M.C., Johansen, S., Kong, F. N., and Westerdahl, H. [2002] Sea Bed Logging (SBL), a new method for remote and direct identification of hydrocarbon filled layers in deepwater areas. *First Break*, **20**, 144-152.

EMGS [2005] Introduction to EMGS and Sea Bed Logging. *EMGS presentation in PETRONAS*, **August**.

Johansen, S.E., Amundsen, H.E.F., Røsten, T., Ellingsrud, S., Eidesmo, T., and Bhuyian, A.H., [2005] Subsurface hydrocarbons detected by electromagnetic sounding. *First Break*, **23**, 1-6.

MacGregor, L. M. [2007] CSEM aids in basalt study. *E & P*, **June**, 71-72.

Mazlan Hj Madon [2007] Geological setting of Sarawak. *The Petroleum Geology and Resources of Malaysia*, **PETRONAS** , 275-283.

Roth, F., Maao, F. A. [2007] Improving Seabed Logging sensitivity in shallow water through Up-Down Separation. *EGM International Workshop*, **April**.

Theresia Heru Kuswardhany [2007] AVO Analysis of the Block F, Rajang Delta, Offshore Sarawak. **March**.

Theresia Heru Kuswardhany, Wong, E. Y., Meor Hakif Amir Hassan, Azwa Jannah, Zuliyana Ibrahim, Nurul Salmi Abudullah [2006] Rajang Delta OJT: Wrapping-up presentation. *Presentation in PMU, PETRONAS*, **April**.